NRL REPORT R-3451

FR-3451

OPTIMUM DESIGN CRITERION FOR SIMULTANEOUS-LOBING ANTENNAS

NAVAL RESEARCH LABORATORY

WASHINGTON, D.C.

NRL REPORT R-3451

OPTIMUM DESIGN CRITERION FOR SIMULTANEOUS-LOBING ANTENNAS

M. L. Kales

April 20, 1949

Approved by:

Dr. L. C. VanAtta, Head, Antenna Research Branch
Dr. J. M. Miller, Superintendent, Radio Division I

NAVAL RESEARCH LABORATORY
CAPTAIN F. R. FURTH, USN, DIRECTOR
WASHINGTON, D.C.

DISTRIBUTION

BuAer	
Attn: Code TD-4	1
Attn: Code EL-51	1
BuOrd	
Attn: Code Re4f	1
BuShips	
Attn: Code 833	2
Dir., USNEL	
Attn: Code 300	2
Cdr., USNOTS	
Attn: Reports Unit	2
CO, USNUSL	
Attn: Mr. C. M. Dunn	1
CO, NADS, Johnsville, Pa.	
Attn: Dr. H. Krutter	1
CO, NADS, Aeronautical Electronic and Electrical Lab.	
Attn: Antenna and Radome Branch	1
CO, SCEL	
Attn: Dir. of Engineering	2
Ch. of Staff, USAF	
Attn: Code AFMEN-2	1
OCSigO	
Attn: SIGGC-2, Rm. 3B-283	2
Attn: Ch. Eng. & Tech. Div., SIGTM-S	1
Dir., ESL	
Attn: Mr. O. C. Woodyard	1
Attn: Mr. Leonard Moore	1
CG, Wright-Patterson Air Force Base	
Attn: MCREEP	1
Attn: MCREEO	1
Attn: MCREER	2
BAGR, Wright-Patterson Air Force Base	
Attn: CADO-D13	1

CONTENTS

ABSTRACT

An investigation is conducted to determine optimum illumination conditions for a simultaneous-lobing antenna consisting of a circular paraboloidal reflector together with a four-horn feed. The E- and H-plane sum and difference patterns of the four-horn feed are calculated as functions of horn size for the favorable case where the apertures of the horns are square and contiguous. The calculated patterns are compared with measured patterns and found to be in very good agreement.

Expressions for the secondary E- and H-plane patterns are obtained in both integral and series forms. Using these results, relative on-axis range and sensitivity are calculated and plotted as functions of $a\Omega/\lambda$, where Ω is one-half the angle subtended at the focus by the reflector, and a/λ is the ratio of the aperture of a single horn to the wavelength. It is found that an antenna designed so that $a\Omega/\lambda = 26^0$, has on-axis range and sensitivity within 5 percent of the maximum values that could be obtained if the antenna were designed to maximize either one alone.

PROBLEM STATUS

This report concludes the work on the problem. Unless otherwise advised, the Laboratory will consider the problem closed one month from the mailing date of this report.

AUTHORIZATION

NRL Problem No. R09-30R

TABLE OF SYMBOLS

V_E	= received E-plane difference signal.
V_H	= received H-plane difference signal.
V_S	= received range signal.
x,y,z	= cartesian coordinates.
ρ,θ,ϕ R,ψ,ξ	= spherical coordinates.
θ_x,θ_y	= angles between the antenna axis and the projections of the radius vector to the target on the E- and H-planes respectively.
α,β	= angles between radius vector to a point on the reflector and the x- and y-axes respectively.
$e(\theta,\phi)$	= single horn pattern.
$e_S(\theta,\phi)$	= feed pattern when the four horns transmit in phase.
$e_e(\theta,\phi)$	= feed pattern when the horn pairs separated by the H-plane are 180° out of phase.
$e_h(\theta,\phi)$	= feed patterns when the horn pairs separated by the E-plane are 180° out of phase.
$e_S'(\theta,\phi)$ $e_e'(\theta,\phi)$ $e_h'(\theta,\phi)$	= calculated feed patterns corresponding to $e_S(\theta,\phi)$, $e_e(\theta,\phi)$, and $e_h(\theta,\phi)$, but neglecting interactions between horns.
$e(\theta),h(\theta)$	= E- and H-plane patterns respectively of single horn.
ϵ	= dielectric constant.
μ	= magnetic permeability.
a,b	= horn aperture dimensions.
j	= $\sqrt{-1}$.
λ	= wavelength.
k	= $2\pi/\lambda$.
K_1,K_2,K_3	= constants.
$\vec{e}_\alpha$	= unit vector in direction of field incident upon the reflector.

$\vec{e}_a$ = unit vector in direction of the reflected field.

$\vec{e}_x, \vec{e}_y, \vec{e}_z$ = unit vectors in the directions of the coordinate axes.

$\vec{e}_\rho$ = unit vector in the direction of the radius vector.

$\vec{e}_n$ = unit vector in the direction of the normal to the reflector.

$\vec{E}_i$ = field incident on the reflector.

$F(\theta,\phi)$ introduced in Equation (8).

$\vec{E}(x,y)$ = reflected field in the aperture of the reflector.

$V_{es}(0)$ = received range signal for target on axis.

$V_{ed}'(0)$ = derivative with respect to angle of received E-plane difference signal when target is on axis.

σ = ± 1

τ = ± 1.

L_e, L_h, M_e, M_h = introduced in Equations (B.23), (B.24), (B.25) and (B.26) respectively.

η = introduced in (B.42)

p = $\sqrt{2\pi a} \sin\theta/\lambda$.

s = $4f/D \tan\theta/2$.

t = $\pi D \sin\psi/2\lambda$.

C_m^n = $\dfrac{n!}{m!(n-m)!}$ $\quad 0 \leq m \leq n$

= 0 if $m < 0$, or $m > n$

f = focal length of the reflector.

D = diameter of the reflector aperture.

$\vec{N}$ introduced in Equation (14).

$E_{p\psi}(\psi,\xi), E_{p\xi}(\psi,\xi)$ introduced in Equations (12) and (13).

$A_o(\theta)$ = $1/2\left\{e(\theta) + h(\theta)\right\}$

$A_2(\theta)$ = $1/2\left\{e(\theta) - h(\theta)\right\}$

v = $\sqrt{(a/2 \sin\theta + 2f \tan\theta/2 \sin\psi)^2 + (a/2 \sin\theta)^2}$

J_n = Bessel function of first kind and order n.

Ω = half the angle subtended by reflector diameter at the focus.

$P(\psi)$, $Q(\psi)$	introduced in Equations (16d) and (16e).
$E_{es}(\psi)$, $E_{hs}(\psi)$	= secondary E- and H-plane sum patterns respectively.
$E_{ed}(\psi)$, $E_{hd}(\psi)$	= secondary E- and H-plane difference patterns respectively.
a_n, b_n	= coefficients in the series expansions for the antenna patterns. (formulas given in Equations (B.56) and (B.57)

OPTIMUM DESIGN CRITERION FOR SIMULTANEOUS-LOBING ANTENNAS

INTRODUCTION

The problem of locating a target, by means of radar, with a high degree of precision involves an accurate determination of the range and bearing of the target. Errors in determining range are inherently low, so that the problem is essentially that of reducing angular errors. One method of doing this is to use a very sharp beam. However, there is a practical limit to the ratio of the aperture size to wavelength upon which the sharpness of the beam depends, not to mention the difficulty of scanning with a very sharp beam. These difficulties are avoided by using some sort of lobe comparison or null system.

Conventional conical-lobing systems suffer from random errors due to fluctuations in the returned signal from the target in the period required for the conical lobing, and from systematic errors due to interference from voltages having the periodicity of the lobing. Even the sequential-lobing system is subject to target and transmitter fluctuations from pulse to pulse. These sources of errors are eliminated by the use of a system which obtains the complete range and error information from each pulse. Such a system is known as a simultaneous-lobing or monopulse system.

Various simultaneous-lobing systems have been analyzed and developed. (See Reference 1.) These differ both in the antenna and in the r-f system, which takes the sums and differences of received signals.

PHYSICAL PRINCIPLES

Simultaneous lobing in one plane may be achieved by two antenna apertures separated in that plane together with an r-f system for taking simultaneously the vector sum and difference of the signals received by the two apertures. For simultaneous lobing in two planes, four apertures may be used with an r-f arrangement for taking sums and differences of the signals received by adjacent pairs.

If the array of apertures is exposed directly to the essentially plane wave received from the target, the signals received by the several apertures will be equal in magnitude, but will differ in phase as the target moves off axis. If the array of apertures is placed in the focal plane of a focusing objective, the signals will differ primarily in amplitude as the target, and therefore the focal spot, moves off axis.

This investigation is concerned with an array of four horns with square contiguous apertures symmetrically located in the focal plane of a paraboloid reflector. The object is to develop optimum design criteria for such a simultaneous-lobing antenna, recognizing

that maximum range and maximum angular sensitivity are both desirable but not necessarily compatible characteristics.

The arrangement of four horns is shown in Figure 1a; the coordinate systems used are indicated in Figure 1b. The x- and y-axes lie in the plane of the horn apertures with the x-axis parallel to the E-vector. The z-axis is parallel to the longitudinal axes of the horns.

On transmission, the power is divided equally between the four horns and all four are in phase, thus providing a single lobe pattern to illuminate the reflector. If energy is reflected back from a target, complex voltages, V_A, V_B, V_C, and V_D, will appear at the throats of the horns. These are then combined by means of suitable r-f circuits to provide voltages represented by:

$$V_E = (V_A + V_B) - (V_C + V_D)$$

$$V_H = (V_A + V_C) - (V_B + V_D)$$

$$V_S = V_A + V_B + V_C + V_D$$

If the target is on the z-axis then V_A, V_B, V_C, V_D will all be equal and hence both V_E and V_H will be zero. If the target is in the xz-plane (i.e., the E-plane), but not on the z-axis, then V_A and V_B will be equal and similarly for V_C and V_D, but V_A and V_C will be unequal. Thus V_H will be zero, but V_E will be different from zero. Moreover, the magnitude of V_E will increase with angular deviation of the target from the axis when the angle is small. Similarly if the target is in the yz- or H-plane but not on the z-axis, V_E will be zero but V_H will be different from zero, and for small angles the magnitude of V_H will increase with angular deviation from the z-axis. If the angular deviation of the target from the z-axis is different from zero in both planes, then both V_E and V_H will be different from zero, and moreover the greater the angular deviations, the greater will be V_E and V_H. For this reason V_E and V_H are referred to as error signals. The radar

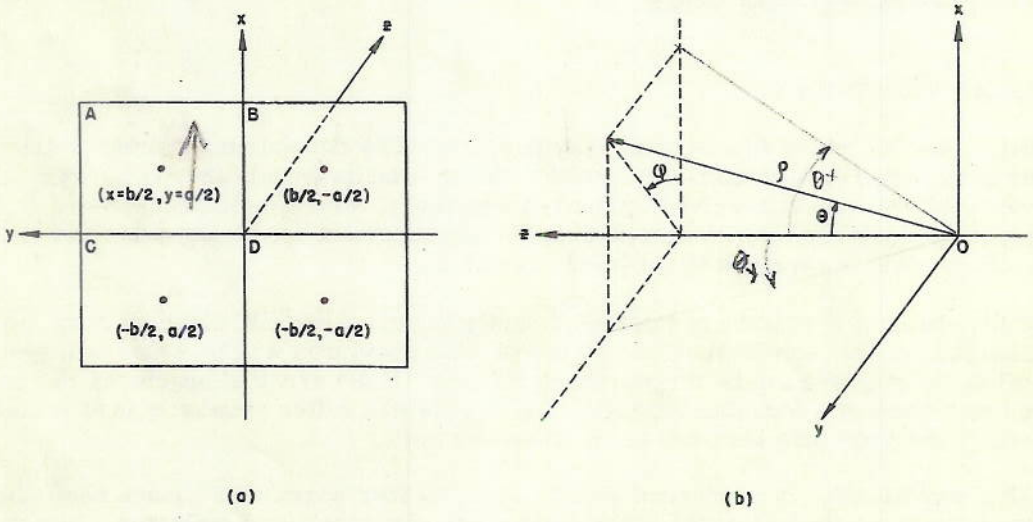

(a) (b)

Fig. 1 - Horn apertures and associated coordinate systems

system may be provided with a tracking device which automatically directs the antenna so as to reduce V_E and V_H to zero. When this is done, the axis of the antenna is directed at the target. The signal V_S is used to provide range information, and a phase standard for establishing the sense of the error information.

Since V_E and V_H are both zero when the antenna axis is pointing directly at the target, deviations from the target are manifested by the appearance of a signal V_E or V_H or both. In order that the deviations be kept small, it is desirable that a small deviation in angle produce large error signals. Let θ_x and θ_y denote the angles between the axis of the antenna and the projections of the radius vector to the target on the E- and H-plane respectively. Then

$$dV_E = \frac{\partial V_E}{\partial \theta_x} d\theta_x + \frac{\partial V_E}{\partial \theta_y} d\theta_y$$

But since V_E is zero whenever the target is in the H-plane it follows that

$$\frac{\partial V_E(0,0)}{\partial \theta_y} = 0$$

Hence

$$dV_E = \frac{\partial V_E}{\partial \theta_x} d\theta_x \quad \text{if } \theta_x = \theta_y = 0$$

and similarly

$$dV_H = \frac{\partial V_H}{\partial \theta_y} d\theta_y \quad \text{if } \theta_x = \theta_y = 0$$

Thus we see that in order to produce large error signals for small angular deviations from the axis, it is necessary that $\partial V_E(0,0)/\partial \theta_x$ and $\partial V_H(0,0)/\partial \theta_y$ be as large as possible. These derivatives are referred to as the E- and H-plane sensitivities of the antenna.

A little consideration will show that range and sensitivity cannot be controlled independently, and that therefore a design which provides for maximum range will not necessarily give maximum sensitivity, and vice versa. To see why, let us refer to Figure 2 and consider what happens in a single plane, say the E-plane.

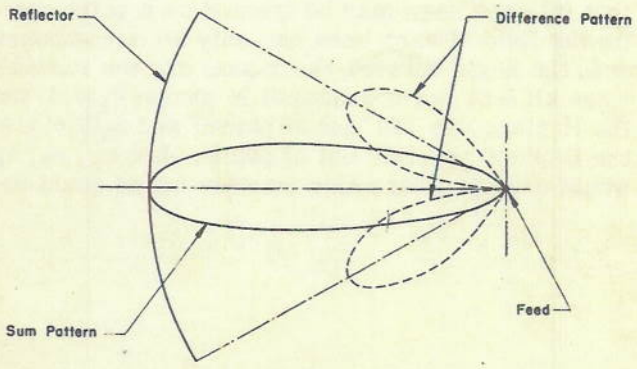

Fig. 2 - Illumination of reflector by sum and difference patterns

On transmission all four horns will be in phase and the reflector will be illuminated by a single-lobe pattern (shown solid in Figure 2). Now it is known that for a constant phase aperture, the gain of the aperture is maximum when the illumination is constant. However, if one attempts to provide an illumination which is very nearly uniform over the reflector, only a small portion of the energy from the feed will be incident upon the reflector, and consequently the over-all gain of the antenna will be low. On the other hand, if a strongly tapered illumination is used, then even though a greater portion of the available energy is intercepted by the reflector, the over-all gain will again be low since the aperture gain is reduced. It has been found that if the intensity of illumination at the edge of the reflector is about 12 db down from the intensity at the center, the gain will be a maximum.

The one-way receiving difference pattern, by the principle of reciprocity, may be analyzed by considering the transmitting pattern when the pair of horns on one side of the H-plane is 180° out of phase with the pair on the other side. In this case the reflector is illuminated by a split beam (shown dotted in Figure 2). It will be seen later that if the horns are designed so that the 10-db point of the single lobe pattern is at the edge of the reflector, then the peaks of the lobes in the split beam will be on the edge of the reflector. This means that the gain in the difference pattern will be low, since a considerable portion of the transmitted power will be spilled over the edge of the reflector. Thus a design which yields maximum gain for the sum pattern will not yield maximum gain for the difference pattern. Reduction of gain in the difference pattern means a reduction in the sharpness of the beam and therefore in the sensitivity. On the other hand, if we try to increase the gain in the difference pattern by designing the horns so that more of the energy in the split beam is intercepted by the reflector, this same design will cause the illumination for the sum pattern to be more strongly tapered, thus leading to a reduction in gain in the sum pattern. It is thus clear that the final design must involve a compromise between maximum possible range and maximum possible sensitivity. In the discussion that follows, the dependence of range and sensitivity on the relative dimensions of the reflector and feed horns will be investigated with a view to obtaining data for an optimum design.

The first part of the discussion will be confined to a study of the primary sum and difference patterns of the four horns alone. In the second part of this report the secondary patterns of the complete antenna consisting of the reflector and four-horn feed are considered.

PRIMARY PATTERNS OF THE FOUR-HORN FEED

In order to render the problem amenable to mathematical calculation, certain simplifying assumptions will be made from time to time. These assumptions have been justified either by experimental data or by mathematical calculation. At the outset we shall assume that (a) each horn may be treated as a point source located at the center of its aperture; (b) the field of each horn has only an α-component which will be denoted by $e(\theta,\phi)$, where α is the angle between the x-axis and the radius vector. Now let $e_s(\theta,\phi)$ denote the field when all four horns transmit in phase; $e_e(\theta,\phi)$ the field when the horn pairs separated by the H-plane are 180° out of phase; and $e_h(\theta,\phi)$ the field when the horn pairs separated by the E-plane are 180° out of phase. Let e'_s, e'_e, e'_h denote the corresponding fields that would exist if interaction between horns could be neglected. Then:

$$e'_s(\theta,\phi) = e(\theta,\phi)\left\{\begin{array}{l} e^{jk\left(\frac{b}{2}\sin\theta\cos\phi+\frac{a}{2}\sin\theta\sin\phi\right)} \\ +e^{jk\left(\frac{b}{2}\sin\theta\cos\phi-\frac{a}{2}\sin\theta\sin\phi\right)} \\ +e^{jk\left(-\frac{b}{2}\sin\theta\cos\phi+\frac{a}{2}\sin\theta\sin\phi\right)} \\ +e^{jk\left(-\frac{b}{2}\sin\theta\cos\phi-\frac{a}{2}\sin\theta\sin\phi\right)} \end{array}\right\}$$

$$= 4e(\theta,\phi)\left[\cos\left(k\frac{a}{2}\sin\theta\sin\phi\right)\cos\left(k\frac{b}{2}\sin\theta\cos\phi\right)\right] \quad (1)$$

$$e'_e(\theta,\phi) = e(\theta,\phi)\left\{\begin{array}{l} e^{jk\left(\frac{b}{2}\sin\theta\cos\phi+\frac{a}{2}\sin\theta\sin\phi\right)} \\ +e^{jk\left(\frac{b}{2}\sin\theta\cos\phi-\frac{a}{2}\sin\theta\sin\phi\right)} \\ -e^{jk\left(-\frac{b}{2}\sin\theta\cos\phi+\frac{a}{2}\sin\theta\sin\phi\right)} \\ -e^{jk\left(-\frac{b}{2}\sin\theta\cos\phi-\frac{a}{2}\sin\theta\sin\phi\right)} \end{array}\right\}$$

$$= 4je(\theta,\phi)\left[\cos\left(k\frac{a}{2}\sin\theta\sin\phi\right)\sin\left(k\frac{b}{2}\sin\theta\cos\phi\right)\right] \quad (2)$$

$$e'_h(\theta,\phi) = e(\theta,\phi)\left\{\begin{array}{l} e^{jk\left(\frac{b}{2}\sin\theta\cos\phi+\frac{a}{2}\sin\theta\sin\phi\right)} \\ -e^{jk\left(\frac{b}{2}\sin\theta\cos\phi-\frac{a}{2}\sin\theta\sin\phi\right)} \\ +e^{jk\left(-\frac{b}{2}\sin\theta\cos\phi+\frac{a}{2}\sin\theta\sin\phi\right)} \\ -e^{jk\left(-\frac{b}{2}\sin\theta\cos\phi-\frac{a}{2}\sin\theta\sin\phi\right)} \end{array}\right\}$$

$$= 4je(\theta,\phi)\left[\sin\left(k\frac{a}{2}\sin\theta\sin\phi\right)\cos\left(k\frac{b}{2}\sin\theta\cos\phi\right)\right] \quad (3)$$

where $k = 2\pi/\lambda$.

At this point the additional assumption is made that

$$\left.\begin{aligned} e_s &= K_1 e'_s \\ e_e &= K_2 e'_e \\ e_h &= K_3 e'_h \end{aligned}\right\} \tag{4}$$

where K_1, K_2, and K_3 are independent of θ and ϕ. The purpose of introducing the constants K_1, K_2, and K_3 is to take into account the effect of the interaction between horns on the gain. Thus it is seen that equations (4) are equivalent to assuming that the interaction between horns does not affect the shape of the resulting patterns, but does effect the gain. The agreement between the calculated patterns and experimental patterns justifies this assumption. The constants K_1, K_2, and K_3 are then determined by the fact that in each case the same total power P_t is transmitted. Thus we have

$$2\sqrt{\frac{\mu}{\epsilon}}\, P_t = \int_0^{2\pi}\int_0^{\pi} K_1^2\, e'_s(\theta,\phi)^2 \sin\theta \, d\theta \, d\phi = \int_0^{2\pi}\int_0^{\pi} K_2^2\, e'_e(\theta,\phi)^2 \sin\theta \, d\theta \, d\phi$$

$$= \int_0^{2\pi}\int_0^{\pi} K_3^2\, e'_h(\theta,\phi)^2 \sin\theta \, d\theta \, d\phi \tag{5}$$

In calculating E-plane and H-plane sum patterns of the four horns, it was found that by the time one had gone beyond the peak of the first side lobe for the four-horn sum pattern, the intensity of the single-horn pattern was less than 15 db down. On the other hand an analysis of the secondary patterns of the feed and reflector shows that both maximum range and sensitivity are reached when the side lobe of the four-horn sum pattern falls outside of the reflector. Thus, for the purposes of this investigation it is sufficient if the single-horn pattern is known only as far as 15 db down. Several empirical formulas are available which describe fairly accurately the E- and H-plane patterns of a horn down to 20 db. If we denote the E- and H-plane patterns respectively by

$$e(\theta) = e(\theta,0) \tag{6a}$$

$$h(\theta) = e\left(\theta,\frac{\pi}{2}\right) \tag{6b}$$

then suitable empirical formulae for $e(\theta)$ and $h(\theta)$ are

$$e(\theta) = \cos(l \sin\theta) \tag{7a}$$

$$h(\theta) = \cos(m \sin\theta) \tag{7b}$$

with the constants l and m chosen to yield the correct 10-db width in each plane. The 10-db widths of horns have been determined experimentally for a large variety of horns, and have been plotted as functions of a/λ and b/λ in a report by Risser (Reference 2).

If a horn with square aperture is used, its H-plane pattern will be broader than its E-plane pattern. When, however, the four horns are combined in a square array, the

principal portion of the resulting E-plane and H-plane patterns are nearly identical. This is because the combined patterns are represented by a product of two factors; one representing the single horn pattern, the other being an array factor which depends on separation between the centers of the horns. The array factor is dominant in determining the principal portions of the combined pattern, and since the centers of the horns are symmetrically distributed, the resulting patterns are very nearly symmetrical. Since symmetry is clearly desirable, this study has been confined to an array of horns with square apertures, and we shall in what follows take b = a.

E- and H-plane sum and difference patterns have been calculated for a range of values of a/λ using equations (1), (2), (3), and (7) and the 10 db widths found in the report by Risser (Ref. 2). The results of these calculations are summarized in a series of graphs.

In order to see how the various patterns depend on the parameter a/λ, all patterns were plotted as functions of $a\theta/\lambda$. The main lobes of the sum patterns in both the E- and H-planes were very nearly identical. The two main lobes shown in Figures 3 and 4 actually represent composite curves for values of λ/a from 0.6 to 1.2, the curves for all intermediate values lying between the two shown. Although the agreement between the difference patterns is not as good, (Figures 5 and 6), the maximum deviation between any two curves in the range is about 1 db over the portion of the pattern of interest. The patterns have not been calculated over the complete range of values of θ, since only the portion of the pattern which is incident upon the reflector enters into the calculations of the secondary patterns. For this reason, only a range of values of θ sufficient to include the first side lobe in the sum pattern was used. As will be seen later, such a range of values of θ is more than enough.

In Figure 7 the E- and H-plane sum and difference patterns are compared for the case $\lambda/a = 1$. This comparison was restricted to the case $\lambda/a = 1$ since corresponding curves in each of the principal planes are very nearly alike over the range of values of λ/a considered. It will be noted that the main lobes of the sum patterns agree closely. As for the difference patterns, the deviation is about 1 db at most up to the value of θ corresponding to the null in the sum pattern. As we shall see later, this includes the main portion of the pattern which is of interest in the calculation of the secondary patterns.

It is interesting to note the presence of high side lobes in the H-plane sum pattern. It is known that a single horn does not have side lobes in the H-plane.

A number of experimental feed patterns were available for comparison with the calculated patterns. These also have been plotted as a function of $a\theta/\lambda$. However, since the centers of the horns were separated by an additional distance equal to twice the wall thickness of the horns, the value of "a" used in plotting was the separation between centers, rather than the aperture of the single horn. Figures 8 and 9 show the experimental E- and H-plane sum patterns together with the calculated pattern for the case $\lambda/a = 1$. Again composite curves were drawn for the principal lobes, and it is again seen that the agreement between calculated and measured patterns is good for the principal lobes. Figures 10 and 11 show the corresponding E- and H-plane difference patterns. Although the agreement here is not as good as it is for the sum patterns, it is still satisfactory. It will be noted that the presence of high side lobes in the H-plane sum patterns is confirmed by the experimental patterns.

Figures 12 and 13 show the E- and H-plane sum and difference patterns, together with the single-horn pattern for the case $\lambda/a = 1$. For values of λ/a between 0.6 and 1.2 it was found that over the range of values of θ which includes the peak of the first side lobe in the sum patterns, the single-horn pattern is not more than 15 db down from its peak.

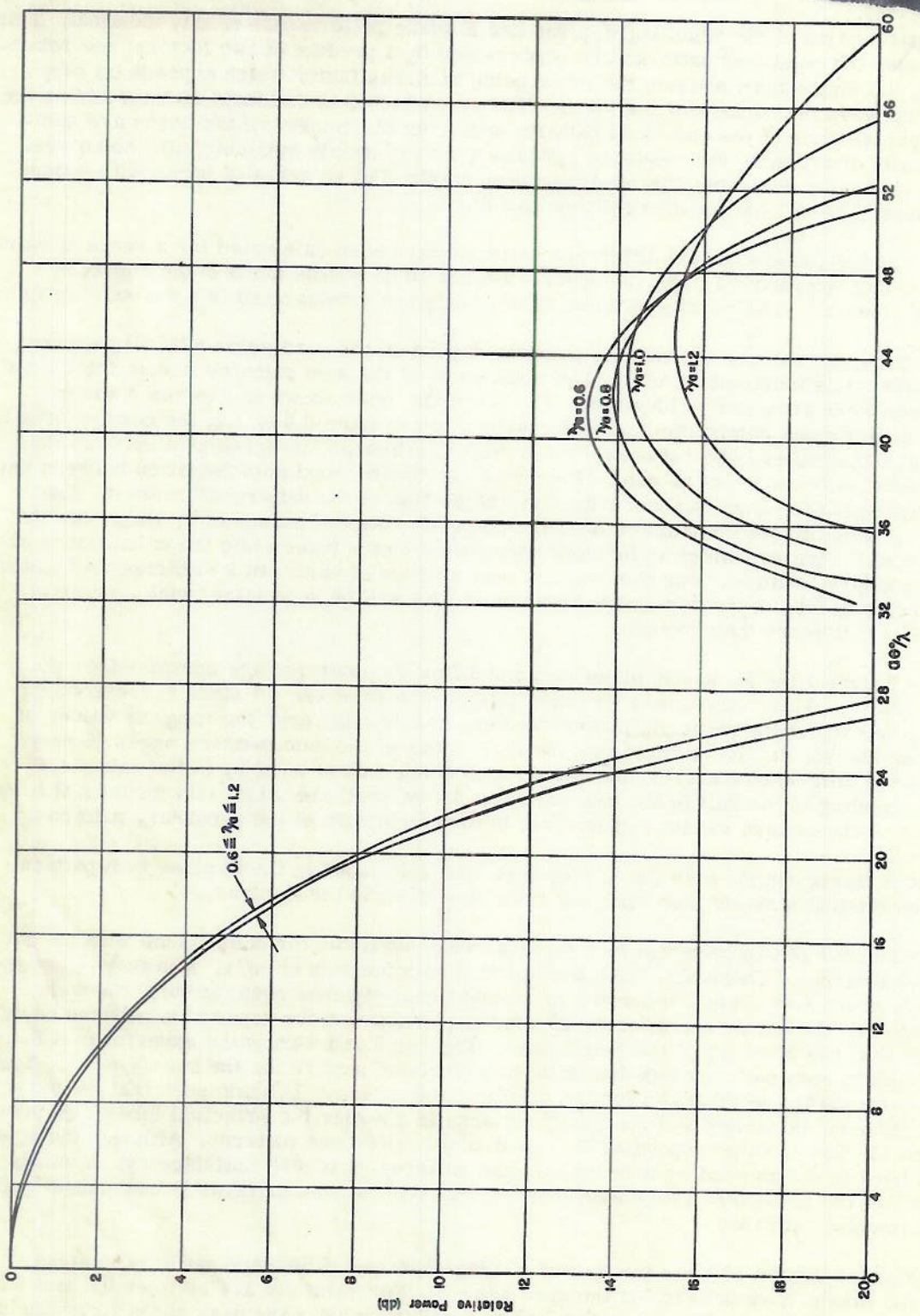

Fig. 3 - Calculated E-plane sum patterns of four-horn feed

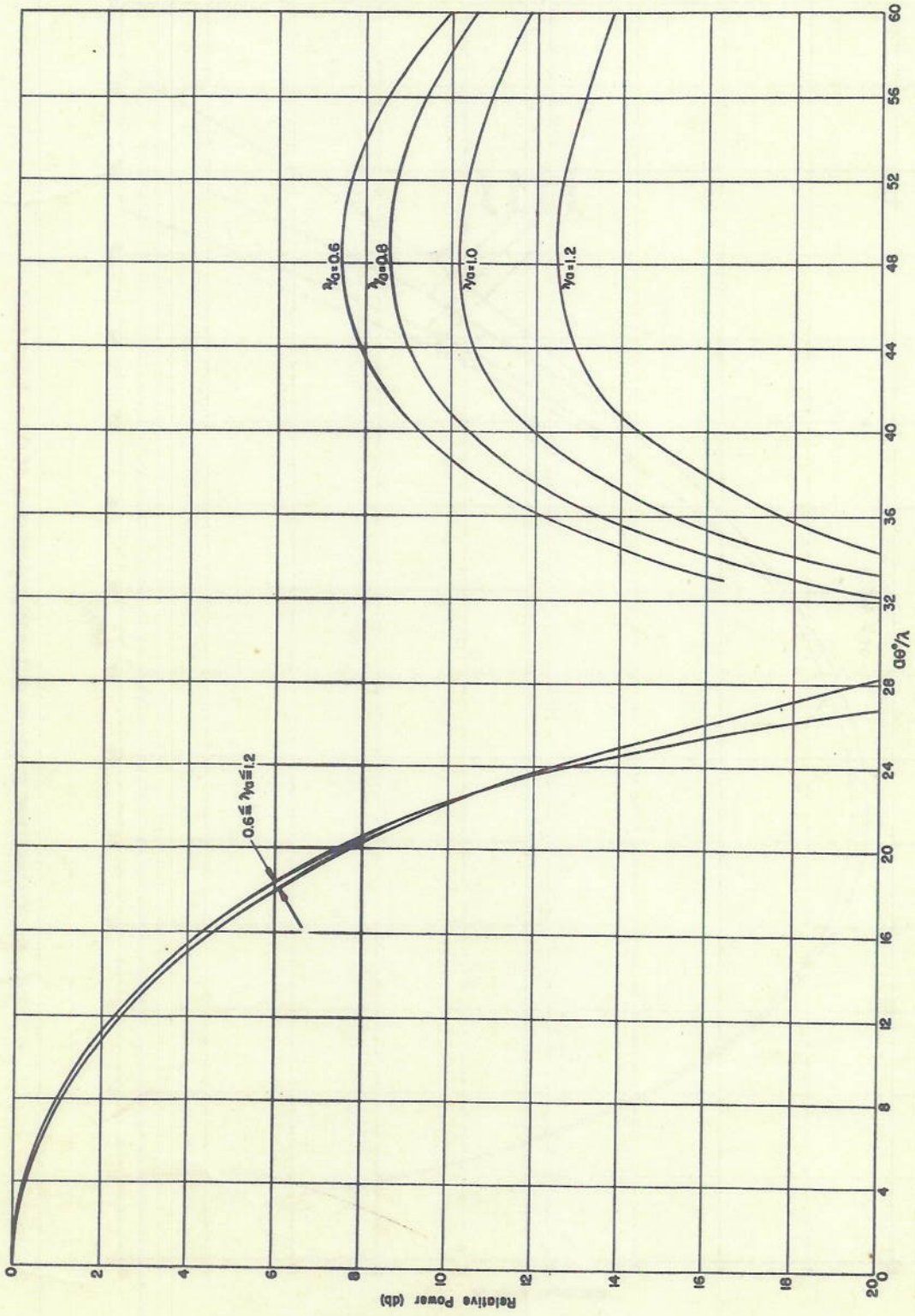

Fig. 4 - Calculated H-plane sum patterns of four-horn feed

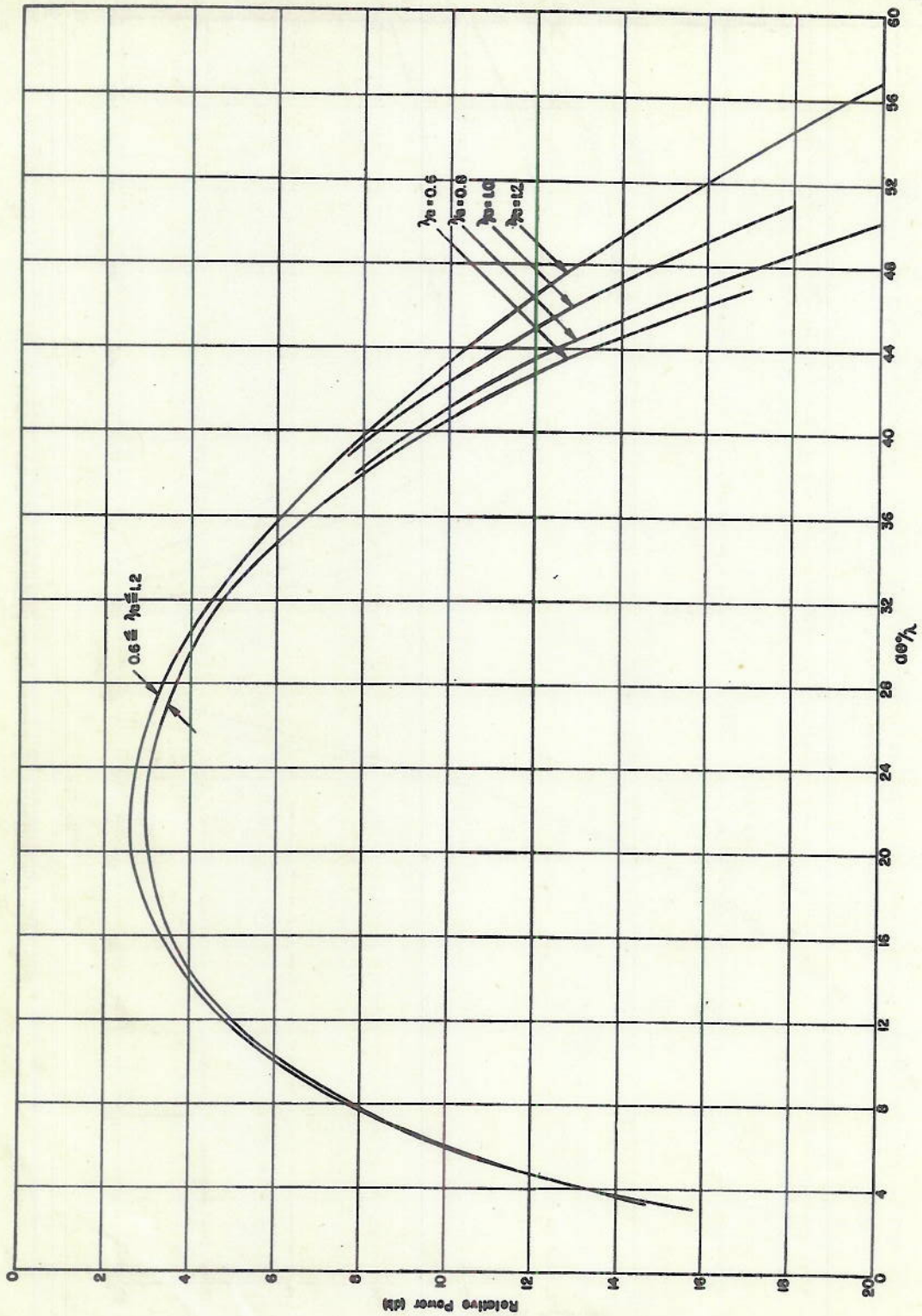

Fig. 5 - Calculated E-plane difference patterns of four-horn feed

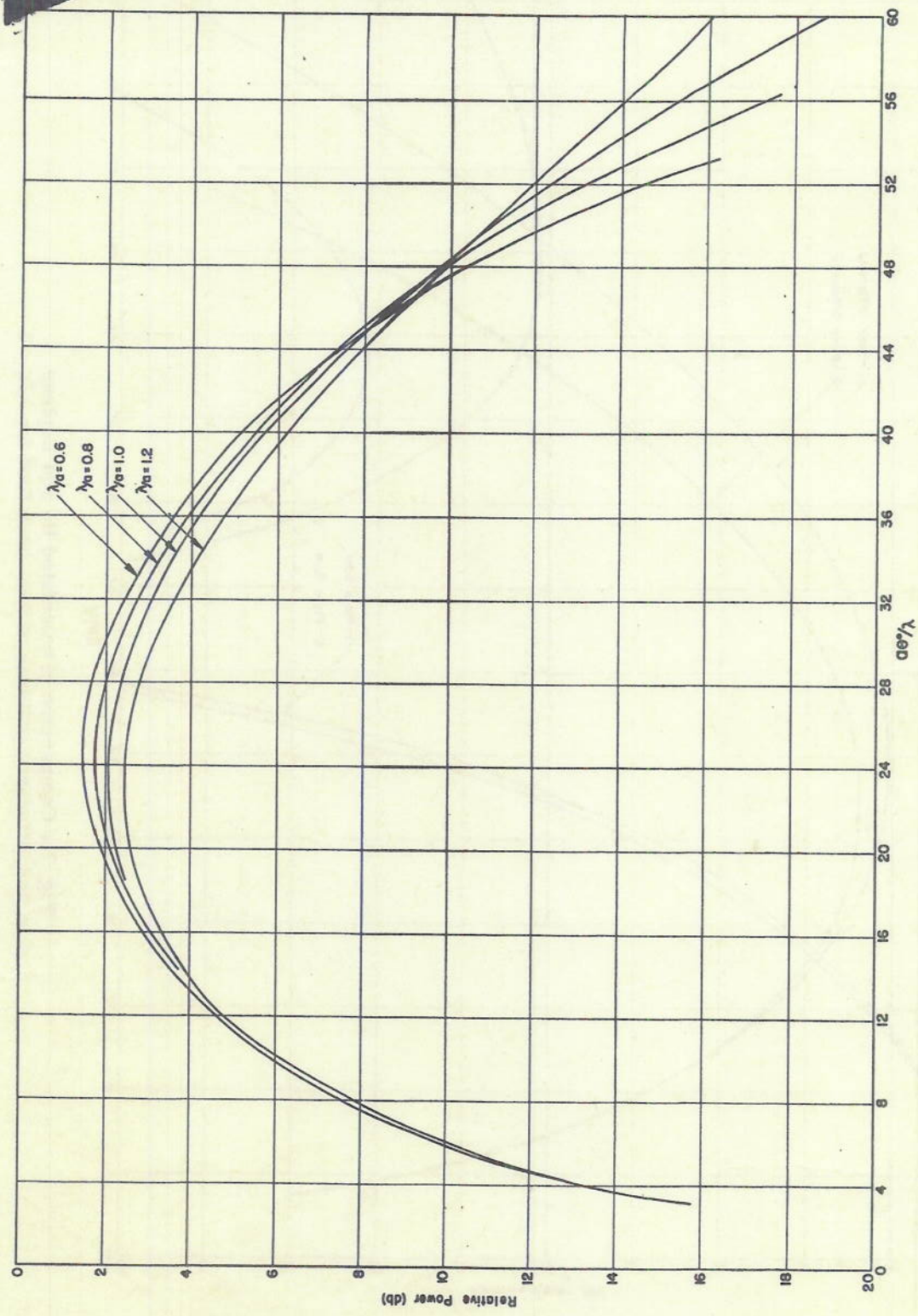

Fig. 6 - Calculated H-plane difference patterns of four-horn feed

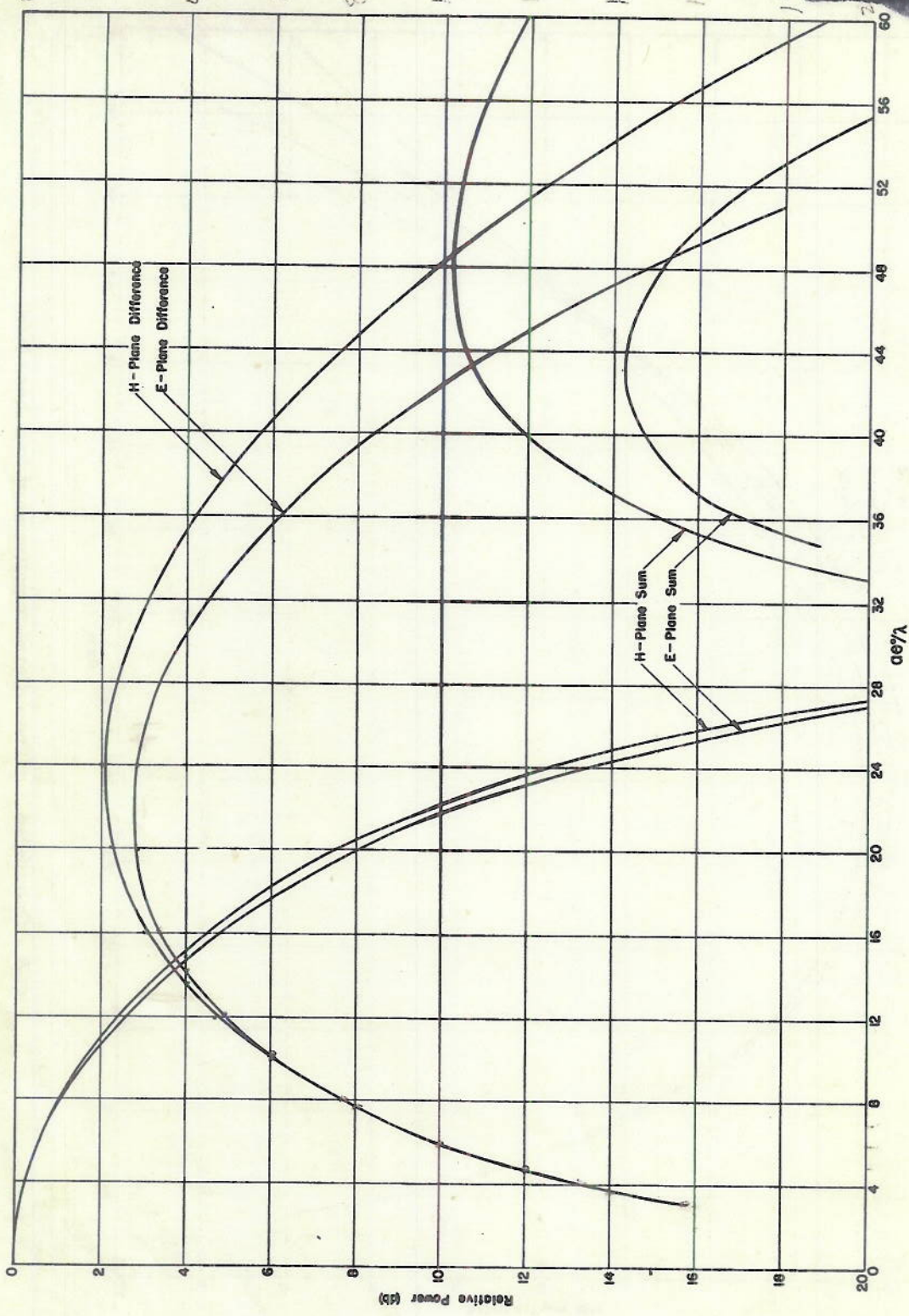

Fig. 7 - Comparison of calculated H- and E-plane sum and difference patterns of four-horn feed for $\lambda/a = 1$

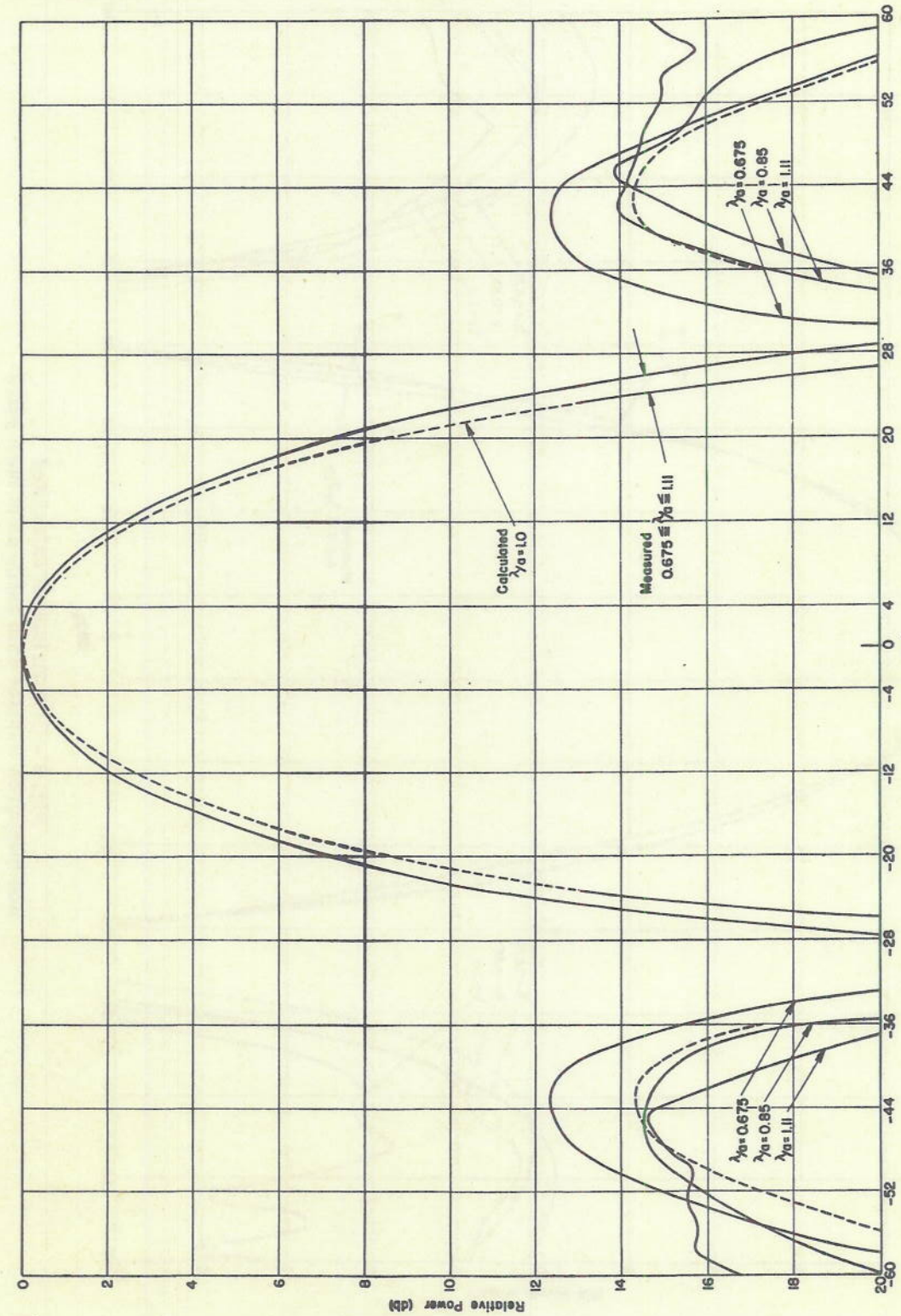

Fig. 8 - Comparison of calculated
and measured E-plane sum patterns of horn pairs

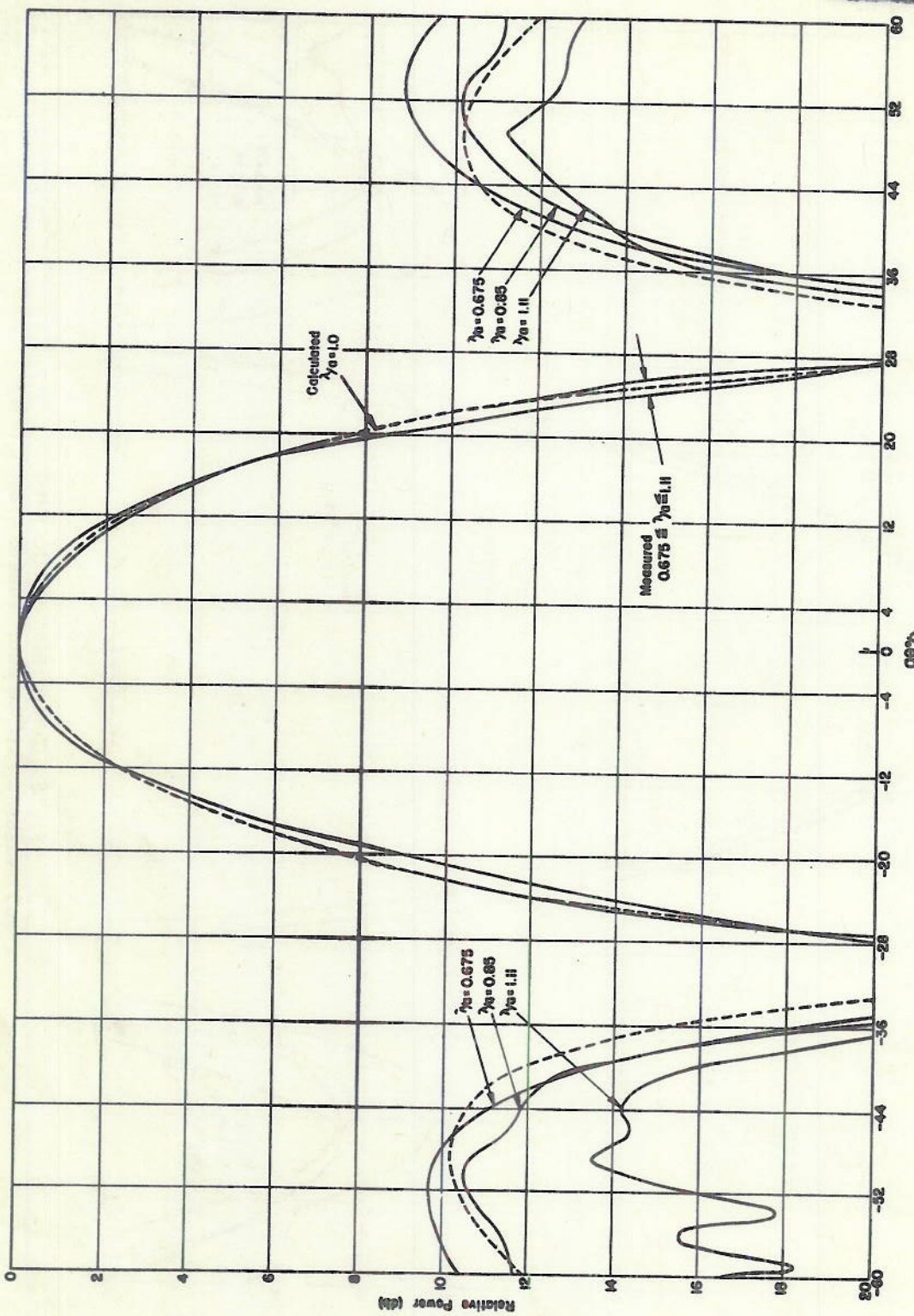

Fig. 9 - Comparison of calculated
and measured H-plane sum patterns of horn pairs

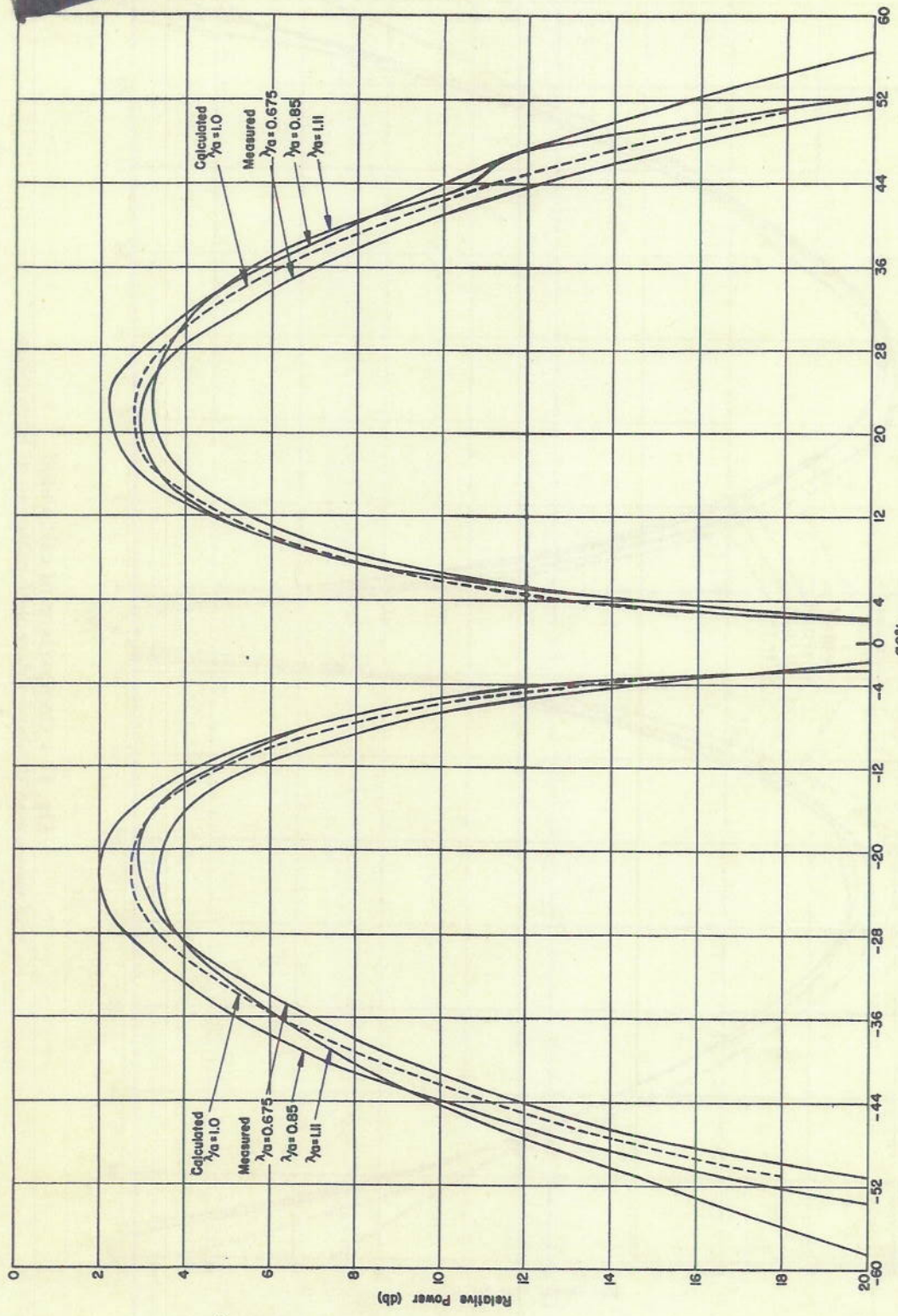

Fig. 10 - Comparison of calculated
and measured E-plane difference patterns of horn pairs

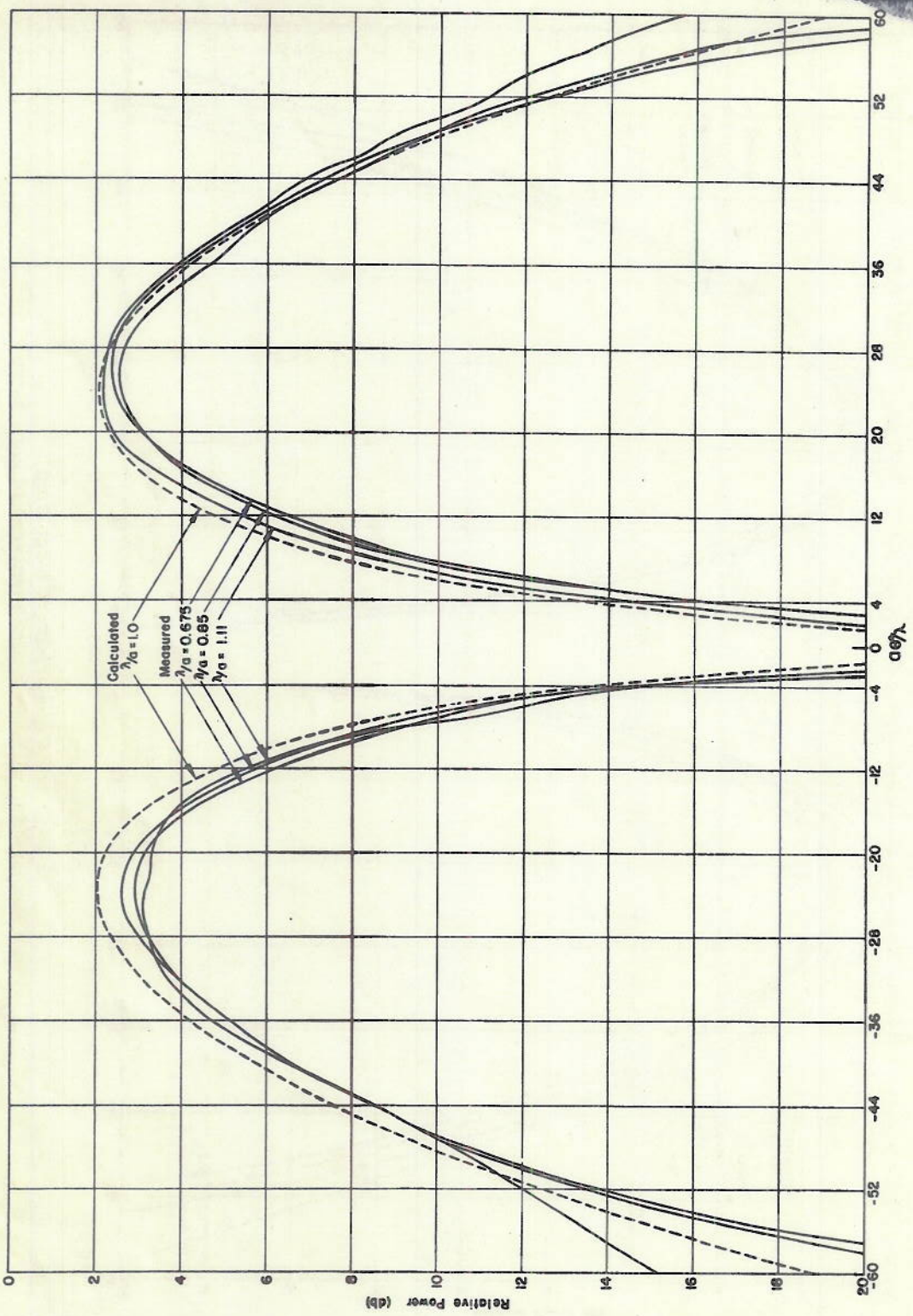

Fig. 11 - Comparison of calculated and measured H-plane difference patterns of horn pairs

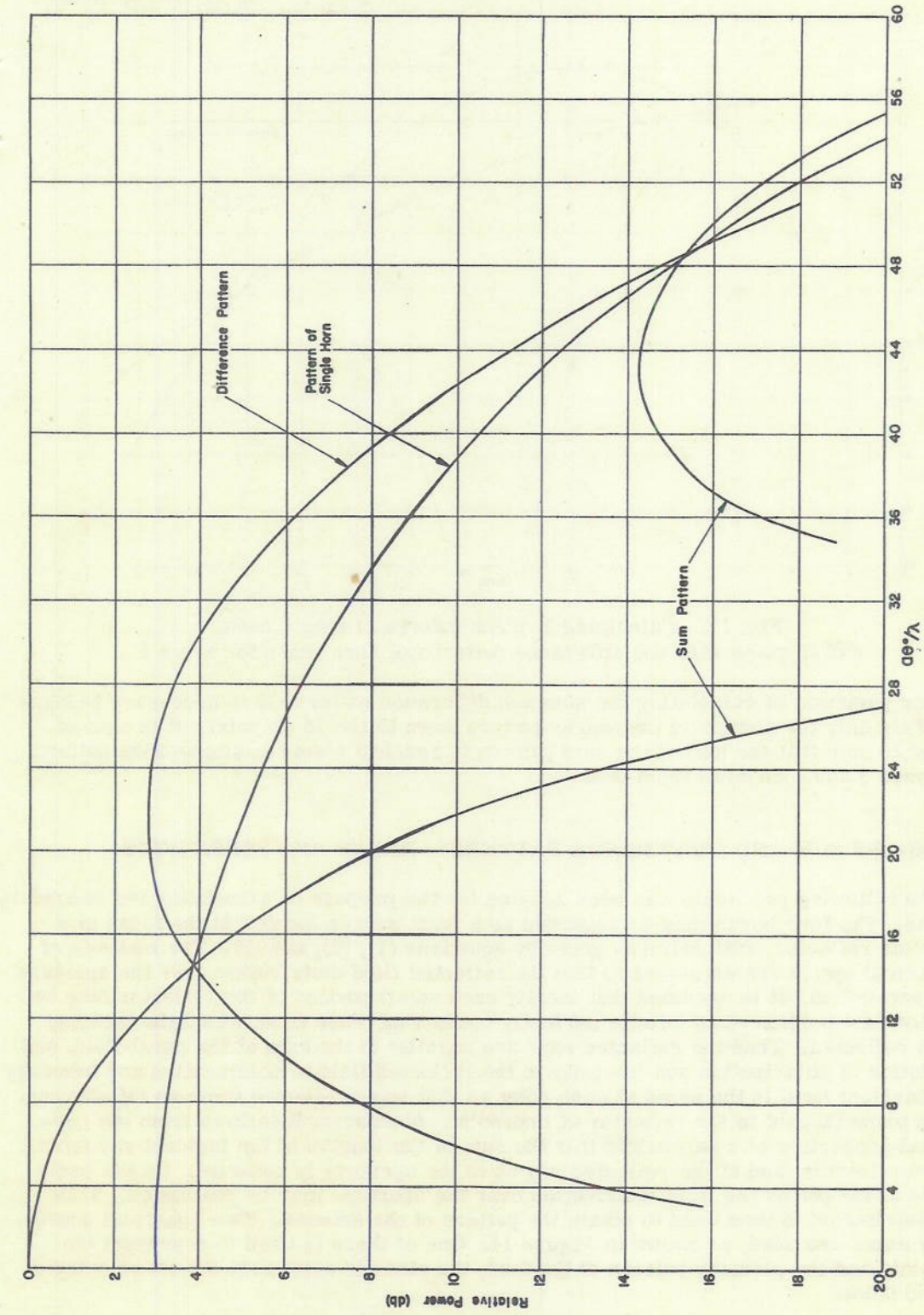

Fig. 12 - Calculated E-plane pattern of single horn, and E-plane sum and difference patterns of horn pairs for $\lambda/a = 1$

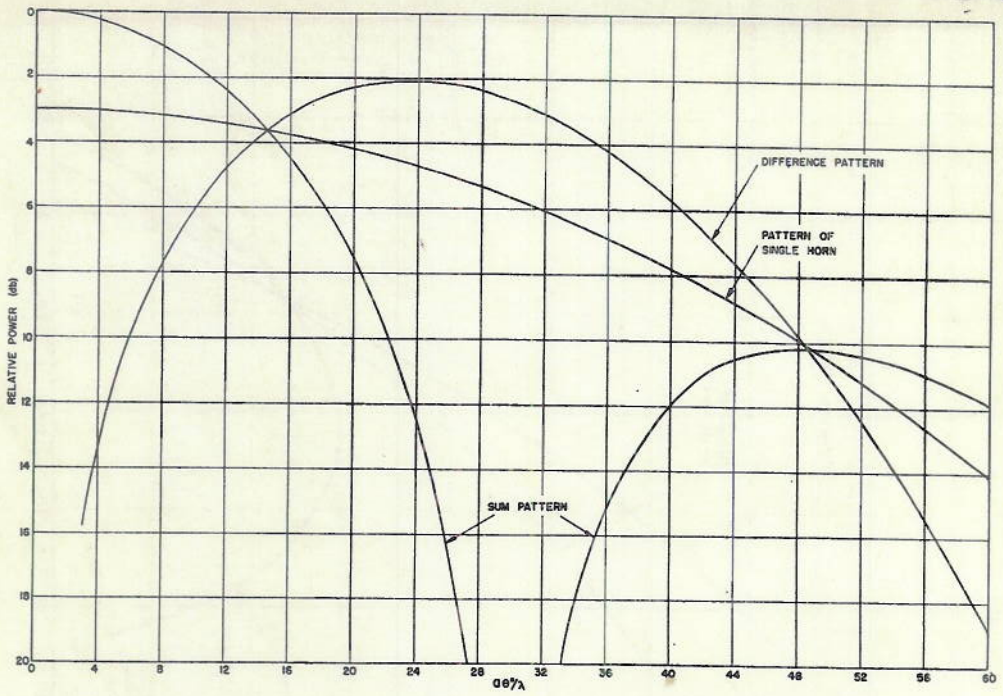

Fig. 13 - Calculated H-plane pattern of single horn, and H-plane sum and difference patterns of horn pairs for $\lambda/a = 1$

Thus for purposes of calculating the sum and difference patterns it is necessary to know accurately only the portion of the single-pattern down to the 15 db point. It is also of interest to note that the null of the sum pattern is reached when the single-horn pattern is between 3 and 4 db down from peak.

SECONDARY SUM AND DIFFERENCE PATTERNS—RANGE AND SENSITIVITY

The following procedure has been adopted for the purpose of calculating the secondary patterns. The four horns may be regarded as a point source located at the focus of a paraboloid reflector, with patterns given by equations (1), (2), and (3). The methods of geometrical optics are employed to find the reflected field distribution over the aperture of the paraboloid. It is assumed that locally each small portion of the reflector may be regarded as a portion of an infinite perfectly conducting plane from which the incident field is reflected. Thus the reflected rays are parallel to the axis of the paraboloid, and the relation of polarization and intensity in the reflected field to polarization and intensity in the incident field is the same at each point as if it were reflected from an infinite conducting plane tangent to the reflector at that point. Moreover, it follows from the geometrical properties of a paraboloid that the sum of the lengths of the incident ray from focus to reflector, and of the reflected ray up to the aperture is constant. On the basis of these assumptions the field distribution over the aperture may be calculated. This field distribution is then used to obtain the pattern of the antenna. Two spherical coordinate systems are used, as shown in Figure 14. One of these is used to represent the paraboloid and the primary pattern of the feed, the other to represent the coordinates of the field point.

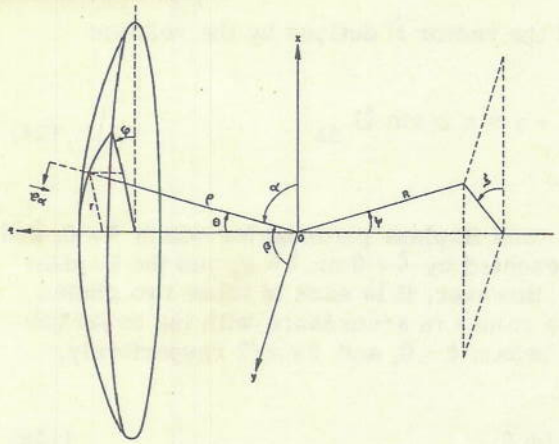

Fig. 14 – Reflector and associated coordinate systems

Now let

$$\vec{E}_i = \frac{F(\theta,\phi)}{\rho} e^{-jk\rho} \vec{e}_\alpha \tag{8}$$

denote the incident field, where $\vec{e}_\alpha$ is a unit vector lying in the plane of the x-axis and the radius, pointing in the direction of increasing α. Then if $\vec{e}_a$ denotes a unit vector in the direction of the reflected field at any point of the reflector, the reflected field is given by

$$\vec{E} = \frac{F(\theta,\phi)}{\rho} e^{-jk\rho} \vec{e}_a \tag{9}$$

In accordance with geometrical optics the reflected field at any point of the aperture will be the same (except for phase) as the reflected field at the point of the paraboloid which lies on the ray through the aperture point. Thus, if x,y denote the coordinates of a point in the aperture, the aperture field is given by

$$\vec{E}(x,y) = \frac{F(\theta,\phi)}{\rho} e^{-j2kf} \vec{e}_a \tag{10}$$

The unit vector $\vec{e}_a$ is parallel to the x,y plane. It will be shown in Appendix A that for sufficiently small values of θ, $\vec{e}_a$ is very nearly equal to $\vec{e}_x$, the unit vector parallel to the x-axis. The following table taken from Appendix A indicates the order of magnitude of the error involved in replacing $\vec{e}_a$ by $\vec{e}_x$ over the aperture. In this table Ω denotes half the angle subtended at the focus by the reflector, and $(\vec{e}_a \cdot \vec{e}_x)_{min}$ represents the minimum value over the aperture of the component of $\vec{e}_a$ in the direction of the x-axis.

Ω	30^0	45^0	52^0	60^0
$(\vec{e}_a \cdot \vec{e}_x)_{min}$	0.997	0.985	0.972	0.943

In all cases the maximum error occurs at the boundary of the aperture. As will be seen later, the calculations will be confined to reflectors for which Ω does not exceed 60^0 by more than a small amount. Hence to a high degree of accuracy we may replace $\vec{e}_a$ by $\vec{e}_x$ and write

$$\vec{E}(x,y) = \frac{F(\theta,\phi)}{\rho} e^{-j2kf} \vec{e}_x \tag{11}$$

Now let $E_p(\psi,\xi)$ denote the radiation field of the antenna. Then the ψ and ξ components of $\vec{E}_p$ are given by (Ref. 3)

$$E_{p\psi}(\psi,\xi) = \frac{jk\, e^{-jkR}}{4\pi} (1 + \cos\psi)(N_x \cos\xi + N_y \sin\xi) \tag{12}$$

$$E_{p\xi}(\psi,\xi) = \frac{-jk\, e^{-jkR}}{4\pi} (1 + \cos\psi)(N_x \sin\xi - N_y \cos\xi) \tag{13}$$

where N_x and N_y are the x and y components of the vector $\vec{N}$ defined by the relation

$$\vec{N} = \int_A \vec{E}(x,y)\, e^{jk\,(x \sin\psi \cos\xi + y \sin\psi \sin\xi)}\, da \tag{14}$$

We shall confine our investigation to the E- and H-plane patterns for which $\xi = 0$, and $\pi/2$ respectively. Actually the E-plane is represented by $\xi = 0$ or $\xi = \pi$, and the H-plane by $\xi = \pi/2$ or $\xi = 3\pi/2$, with ψ always positive. However, if in each of these two planes we allow ψ to assume both positive and negative values in accordance with the usual conventions, then we can restrict ourselves to the values $\xi = 0$, and $\xi = \pi/2$ respectively. We shall denote the E- and H-plane patterns by

$$E_e(\psi) = E_{p\psi}(\psi,0) \tag{15a}$$

$$E_h(\psi) = E_{p\xi}(\psi,\pi/2) \tag{15b}$$

The E- and H-plane sum and difference patterns can be calculated by substituting for the function $\vec{E}(x,y)$ in (14) the aperture distributions which are obtained from the corresponding sum and difference patterns of the feed.

The details of the calculations are presented in Appendix B. Let

$$A_0(\theta) = \frac{1}{2}\left\{e(\theta) + h(\theta)\right\} \tag{16a}$$

$$A_2(\theta) = \frac{1}{2}\left\{e(\theta) - h(\theta)\right\} \tag{16b}$$

$$v^2 = \left(\frac{a}{2}\sin\theta + 2f\tan\frac{\theta}{2}\sin\psi\right)^2 + \left(\frac{a}{2}\sin\theta\right)^2 \tag{16c}$$

$$P(\psi) = 2\pi\int_0^{\Omega} A_0(\theta)\tan\frac{\theta}{2}\,J_0(kv)\,d\theta \tag{16d}$$

$$Q(\psi) = 2\pi\int_0^{\Omega} A_2(\theta)\tan\frac{\theta}{2}\left\{(a\sin\theta)^2/2v^2 - 1\right\}\,J_2(kv)\,d\theta \tag{16e}$$

Let $E_{es}(\psi)$ and $E_{hs}(\psi)$ denote the E- and H-plane sum patterns, and $E_{ed}(\psi)$ and $E_{hd}(\psi)$ denote the E- and H-plane difference patterns, with a common phase factor $j \exp\left\{-jk(R + 2f)\right\}$ omitted. Then it is shown that

$$E_{es}(\psi) = 4\frac{K_1 D}{\lambda}\cdot\frac{f}{D}\left\{P(\psi) + P(-\psi) + Q(\psi) + Q(-\psi)\right\} \tag{17a}$$

$$E_{hs}(\psi) = 4\frac{K_1 D}{\lambda}\cdot\frac{f}{D}\left\{P(\psi) + P(-\psi) - Q(\psi) - Q(-\psi)\right\} \tag{17b}$$

$$E_{ed}(\psi) = 4\frac{K_2 D}{\lambda} \cdot \frac{f}{D} \left\{ P(\psi) - P(-\psi) + Q(\psi) - Q(-\psi) \right\} \tag{17c}$$

$$E_{hd}(\psi) = 4\frac{K_3 D}{\lambda} \cdot \frac{f}{D} \left\{ P(\psi) - P(-\psi) - Q(\psi) + Q(-\psi) \right\} \tag{17d}$$

In order to see how the gain and sensitivity vary with the aperture illumination, we shall assume that the aperture diameter D is held constant, and the size of the feed is kept fixed, but Ω, or in other words f/D, is varied. In this way various portions of the feed pattern are intercepted by the reflector, and the gain and sensitivity will vary accordingly. In practice, however, the reverse procedure is generally followed. One usually starts with a reflector of given diameter D and f/D ratio, and tries to select a suitable feed which will give optimum gain and sensitivity. From physical considerations, it seems intuitively obvious that the antenna patterns will depend primarily on the field distribution over the aperture. Thus it appears that the results that are obtained should be independent of whether a given aperture field distribution is produced by varying the f/D ratio with the feed size fixed, or varying the feed size with the f/d ratio held constant. A semi-quantitative proof of this statement is given in Appendix C.

If we let $t = \pi D \sin \psi/2\lambda$, the functions $P(\psi)$ and $Q(\psi)$ can be expanded in series in powers of t. Substitution of these series in equations (17) leads to the following equations for the fields:

$$E_{es}(\psi) = K_1 D/\lambda \sum_{n=0}^{\infty} (a_{2n} + b_{2n})\, t^{2n} \tag{18a}$$

$$E_{hs}(\psi) = K_1 D/\lambda \sum_{n=0}^{\infty} (a_{2n} - b_{2n})\, t^{2n} \tag{18b}$$

$$E_{ed}(\psi) = K_2 D/\lambda \sum_{n=0}^{\infty} (a_{2n+1} + b_{2n+1})\, t^{2n+1} \tag{18c}$$

$$E_{hd}(\psi) = K_3 D/\lambda \sum_{n=0}^{\infty} (a_{2n+1} - b_{2n+1})\, t^{2n+1} \tag{18d}$$

If a/λ is held fixed, the coefficients a_n and b_n depend only on the parameter Ω. The expressions for these coefficients are given in equations (B.56) and (B.57) Appendix B.

Let us consider now how the received range and error signals vary with angle ψ in the E-plane, assuming that the four horns are in phase on transmission. After reflection from the target, the power received in the range channel will be proportional to $E_{es}^4(\psi)$, and the power received in the difference channel will be proportional to $E_{es}^2(\psi)\, E_{ed}^2(\psi)$. The corresponding input voltages will be proportional to $E_{es}^2(\psi)$ and $E_{es}(\psi) \cdot E_{ed}(\psi)$ respectively. Thus, the on-axis range signal is proportional to $E_{es}^2(0)$, and the sensitivity which is defined as the angular derivative of the error signal evaluated for $\psi = 0$ is

proportional to

$$\frac{d}{d\psi} E_{es}(\psi)\, E_{ed}(\psi)\Big]_{\psi = 0}$$

Since $E_{es}(\psi)$ attains its maximum value at $\psi = 0$, $E_{es}'(0) = 0$. Hence

$$\frac{d}{d\psi} E_{es}(\psi)\, E_{ed}(\psi)\Big]_{\psi = 0} = E_{es}(0)\, E_{ed}'(0)$$

We now wish to determine the value of Ω which makes $E_{es}^2(0)$ a maximum, and the value of Ω which makes the sensitivity, or in other words, $E_{es}(0)\, E_{ed}'(0)$ a maximum. (It will be recalled that for a given feed, the illumination over the reflector is determined by the value of Ω.)

From (18a) and (18c) we see that

$$E_{es}(0)^2 = K_1^2 (D/\lambda)^2 a_0(\Omega)^2 \tag{19}$$

$$E_{ed}'(0) = \frac{\pi}{2} K_2 (D/\lambda)^2 \left\{a_1(\Omega) + b_1(\Omega)\right\} \tag{20}$$

Thus, as we vary Ω and hold D/λ and a/λ constant, we find that

$$E_{es}^2(0) \sim a_0(\Omega)^2 \tag{21}$$

$$E_{es}(0)\, E_{ed}'(0) \sim a_0(\Omega) \left\{a_1(\Omega) + b_1(\Omega)\right\} \tag{22}$$

The coefficients $a_0(\Omega)$, $a_1(\Omega)$, and $b_1(\Omega)$ may be obtained by numerical integration, and the resulting expressions for maximum range signal and sensitivity plotted as a function Ω. The values of Ω for which these quantities are a maximum can then be obtained from the graphs.

The expressions for maximum range and sensitivity have been obtained as functions of Ω, with a/λ held constant. However, if a/λ as well as Ω is allowed to vary, the maximum range and sensitivity become functions of both Ω and a/λ. In the light of earlier remarks, it would be expected that each of these quantities could be expressed as a function of $a\Omega/\lambda$. In order to check this conclusion, the calculated values of sensitivity and "on-axis" range were plotted as functions of $a\Omega/\lambda$ for values of $a/\lambda = 0.8$, 1.0, 1.1, and 1.2, and it was found that the corresponding curves obtained for each of these values of a/λ were practically coincident. Figure 15 shows the graphs of sensitivity and on-axis range as functions of $a\Omega/\lambda$ for the case where $a/\lambda = 1$, plotted in percent. On the same figure the illumination of the E-plane sum pattern of the four-horn feed is plotted in db as a function of $a\theta/\lambda$. If we set $\theta = \Omega$, we are thus able to find how many db down from peak the illumination is at the edge of the reflector, when the reflector subtends on angle 2Ω at the focus. This then gives us a correspondence between sensitivity and on-axis range on the one hand, and the illumination in the sum pattern at the edge of the reflector on the other hand.

From the figure it is seen that the on-axis range attains its maximum value when $a\Omega/\lambda = 23^\circ$. This corresponds to an illumination which is down 12 db at the edge of the reflector. Maximum sensitivity occurs at $a\Omega/\lambda = 29^\circ$. This corresponds to the case where we are almost down to the null of the sum pattern at the edge of the reflector.

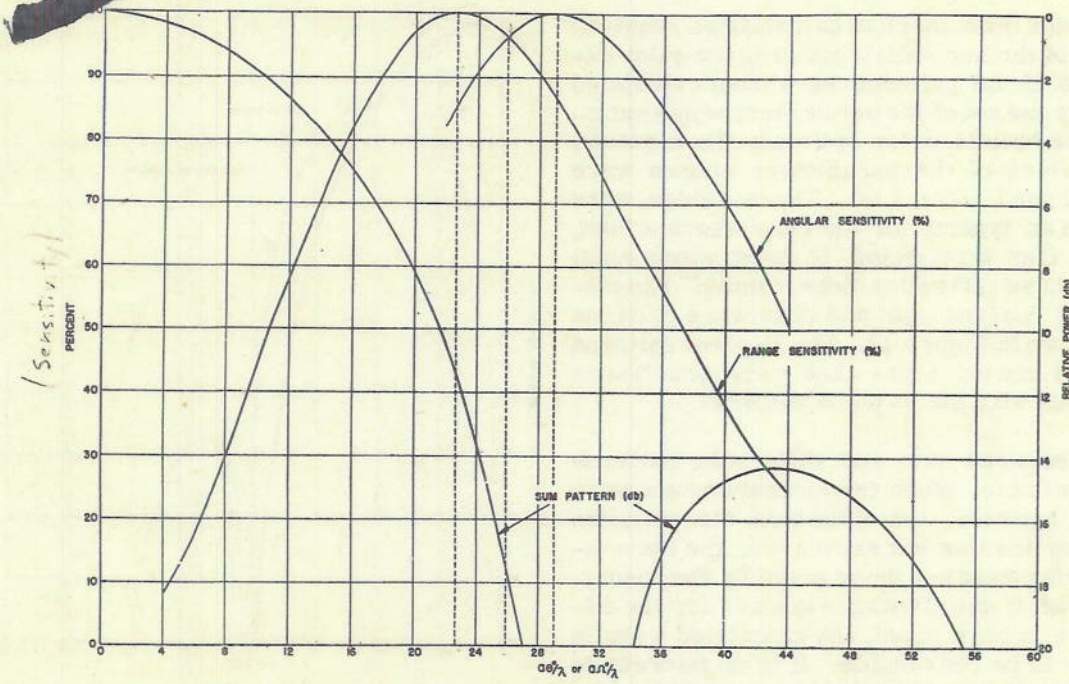

Fig. 15 - Calculated value of range and sensitivity in E-plane as a function of $a\Omega^{\circ}/\lambda$ in percent of maximum. Calculated E-plane sum pattern of four-horn feed as a function of $a\Omega^{\circ}/\lambda$

(The null will fall at the edge of the reflector when $a\Omega/\lambda = 30^{\circ}$.) It will be noted that the sensitivity and on-axis range curves vary slowly with Ω in the neighborhoods of their respective maxima. The two curves intersect when $a\Omega/\lambda = 26^{\circ}$. For this value of Ω, both the sensitivity and on-axis range are down only 3.5 percent from their respective maxima. This, then, would appear to be a suitable operating point. The illumination in the sum pattern of the feed, corresponding to this value of $a\Omega/\lambda$, would be down about 18 db at the edge of the reflector.

By way of illustration, let us assume that the f/D ratio of the reflector is 1. Then from the relation $\tan \Omega/2 = D/4f$ we find that $\Omega \cong 28^{\circ}$. Substituting in the formula $a\Omega/\lambda = 26^{\circ}$, we find that $a/\lambda = 0.93$. This determines the size of the horns to be used.

H-plane sensitivity curves have also been claculated, but have not been shown here since they were found to differ only slightly from the E-plane sensitivity curves. The H-plane sensitivity is given by the relation

$$E_{hs}(0)\, E_{hd}'(0) \sim a_0(\Omega) \left\{ a_1(\Omega) - b_1(\Omega) \right\}$$

Comparing with (22), which gives the E-plane sensitivity, it is clear that the two sensitivities should be very nearly alike provided $b_1(\Omega)$ is small compared to $a_1(\Omega)$. The calculations show this to be the case. This is not surprising, for if one examines (B.56) and (B.57) in Appendix B, it will be seen that the expressions for $a_1(\Omega)$ and $b_1(\Omega)$ differ essentially in the factors $A_0(\theta)$ and $A_2(\theta)$ which appear under the integral sign. However, $A_2(\theta)$ is small compared to $A_0(\theta)$, since $A_0(\theta)$ represents half the sum of the E- and H-plane patterns of the single horn, and $A_2(\theta)$ represents half the difference.

Since the numerical calculations required to obtain the secondary patterns are quite extensive, these patterns have been calculated for only one set of the parameters which satisfied the criterion for optimum illumination. The values of the parameters chosen were $a/\lambda = 1$, and $f/D = 1.08$. These values were chosen as typical for the case where a lens, rather than a reflector, is used, since most lenses have f/D ratios close to unity. The calculated E-plane sum and difference patterns are shown in Figure 16. The H-plane patterns are not shown, since they were practically identical with the E-plane patterns.

Measured sum and difference patterns are available. When the measurements were taken, however, the criterion for optimum illumination was not known, and the horn dimensions were not those given by the theory. However, if due allowance is made for the difference in horn sizes, the calculated results appear to be reasonable. It is of interest to note that the width at half-power of the sum pattern is $1.2\,\lambda/D$, the value that one would expect for an illumination which is 18 db down at the edge of the reflector.

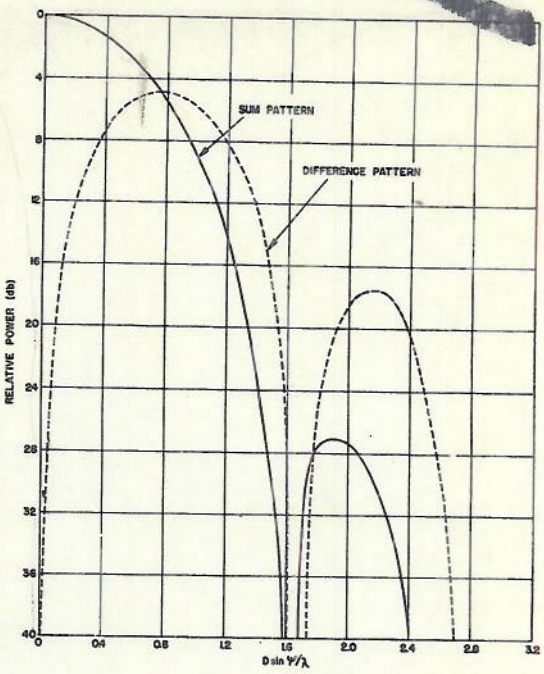

Fig. 16 - Sum and difference patterns for case $a/\lambda = 1$, $a\Omega/\lambda = 26^\circ$

It was stated earlier in this report that the maximum value of Ω which would enter into consideration would not greatly exceed 60°. To see this, let us recall that if b denotes the width of the waveguide, then in order to insure propagation of the fundamental mode we must have $\lambda < 2b$, or $\lambda/b < 2$. Now since $a \geq b$, we also have $\lambda/a < 2$. But from Figure 15 it can be seen that both maximum range and maximum sensitivity are reached for $a\Omega/\lambda < 30^\circ$, or $\Omega < (\lambda/a)\, 30^\circ < 60^\circ$.

CONCLUDING REMARKS

We have seen that when a paraboloidal reflector is illuminated by a feed consisting of four, square, contiguous horns associated with a proper r-f system, the angular aperture of the reflector should be related to the aperture of the single horn by the formula

$$a\Omega/\lambda = 26^\circ$$

where Ω is half the angle subtended by the reflector at the focus, and a is the aperture of a single horn. If the antenna is so designed, the on-axis range and both the E-plane and H-plane sensitivities will be within 5 percent of the maximum values that could be obtained if the antenna were designed to maximize any one of these quantities. Moreover, corresponding E-plane and H-plane sum or difference patterns will be almost identical.

The criterion for optimum design can be expressed in another way. From Figure 15 it is seen that if the feed is designed so that its sum pattern is between 17 and 18 db down at the edge of the reflector the criterion for optimum results will be obtained. The size of horns for which the primary sum pattern will be a given number of db down at the edge of the reflector can be obtained from Figure 3.

The analysis in this report has been based on the use of a paraboloidal reflector as the focusing objective. Physically, it seems clear that the secondary patterns depend only on the amplitude and phase distribution over the aperture of the focusing objective. The amplitude and phase distribution over the aperture of a properly designed lens should differ only slightly from that of a paraboloidal reflector. Hence, it seems reasonable to assume that the criterion for optimum illumination which was derived for the case of a paraboloidal reflector will apply as well to an antenna which employs a lens.

It should be pointed out that in developing this theory it was assumed that the spacing between horn centers was equal to the size of the single horn apertures. Hence, for proper design, the wall thickness of the horns should be reduced to zero at the edges of the apertures where they come in contact. If this is impractical, the value of "a" in the expression $a\Omega/\lambda$ should be taken as the distance between horn centers rather than the horn aperture, since, as was pointed out earlier, the spacing between centers is more critical than the horn aperture in its effect on the patterns.

ACKNOWLEDGMENT

The author wishes to express his gratitude to Dr. L. J. Chu and Dr. L. C. VanAtta for their many valuable suggestions and constant encouragement.

The experimental work on the primary feed patterns was done by Mr. Cleveland Hopkins.

* * *

APPENDIX A

Proof That the X-Component of $\vec{e}_a$ is Very Nearly Equal to Unity

Let $\vec{e}_x$, $\vec{e}_y$, $\vec{e}_z$ denote unit vectors in the direction of the coordinate axes; $\vec{e}_\rho$, a unit vector in the direction of the radius; $\vec{e}_n$, a unit vector in the direction of the normal to the paraboloid and pointing towards the focus side of the paraboloid; $\vec{e}_\alpha$ a unit vector in the direction of the incident field; and $\vec{e}_a$ a unit vector in the direction of the reflected field. An expression for $\vec{e}_a \cdot \vec{e}_x$ is obtained, and it is shown that its minimum value over the aperture differs only slightly from unity.

The vector $\vec{e}_a$ is given by the formula (Ref. 4)

$$\vec{e}_a = 2(\vec{e}_n \cdot \vec{e}_\alpha)\, \vec{e}_n - \vec{e}_\alpha \tag{A.1}$$

The equation of the paraboloid (see Figure 14) is:

$$x^2 + y^2 = 4f(f - z) \tag{A.2}$$

The components of $\vec{e}_n$ are then proportional to x, y, 2f. Hence

$$\vec{e}_n = \frac{-x}{\sqrt{x^2 + y^2 + 4f^2}}\,\vec{e}_x - \frac{y}{\sqrt{x^2 + y^2 + 4f^2}}\,\vec{e}_y - \frac{2f}{\sqrt{x^2 + y^2 + 4f^2}}\,\vec{e}_z \tag{A.3}$$

In spherical coordinates

$$\begin{aligned} x &= \rho \sin\theta \cos\phi \\ y &= \rho \sin\theta \sin\phi \\ z &= \rho \cos\theta \end{aligned} \tag{A.4}$$

and the equation of the paraboloid is given by

$$\rho = f \sec^2 \theta/2 \tag{A.5}$$

Thus

$$x^2 + y^2 = \rho^2 \sin^2\theta = f^2 \sec^4 \theta/2 \sin^2\theta = 4f^2 \tan^2 \theta/2 \tag{A.6}$$

and

$$x^2 + y^2 + 4f^2 = 4f^2(1 + \tan^2 \theta/2) = 4f^2 \sec^2 \theta/2 \tag{A.7}$$

Also from Figure 14

$$\begin{aligned} x &= \rho \cos\alpha = f \sec^2 \theta/2 \cos\alpha \\ y &= \rho \cos\beta = f \sec^2 \theta/2 \cos\beta \end{aligned} \tag{A.8}$$

and

$$\cos \alpha = \sin \theta \cos \phi$$
$$\cos \beta = \sin \theta \sin \phi \qquad \text{(A.9)}$$

Substituting (A.7) and (A.8) in (A.3) gives

$$\vec{e}_n = \frac{1}{2 \sec \theta/2} \left\{ - \sec^2 \theta/2 \cos \alpha \, \vec{e}_x - \sec^2 \theta/2 \cos \beta \, \vec{e}_y - 2 \vec{e}_z \right\} \qquad \text{(A.10)}$$

The unit vectors $\vec{e}_x$, $\vec{e}_\rho$, and $\vec{e}_\alpha$ lie in a plane, and the vector $\vec{e}_\rho$ makes an angle α with $\vec{e}_x$.

From Figure 17 (see page 30) it is seen that

$$\vec{e}_\alpha = \vec{e}_\rho \cot \alpha - e_x \csc \alpha = \frac{\vec{e}_\rho \cos \alpha - \vec{e}_x}{\sin \alpha} \qquad \text{(A.11)}$$

But

$$\vec{e}_\rho = \cos \alpha \, \vec{e}_x + \cos \beta \, \vec{e}_y + \cos \theta \, \vec{e}_z \qquad \text{(A.12)}$$

Substituting in (A.11)

$$\vec{e}_\alpha = \frac{1}{\sin \alpha} \left\{ - \sin^2 \alpha \, \vec{e}_x + \cos \alpha \cos \beta \, \vec{e}_y + \cos \alpha \cos \theta \, \vec{e}_z \right\} \qquad \text{(A.13)}$$

Thus:

$$\vec{e}_n \cdot \vec{e}_\alpha = \frac{1}{2 \sec \theta/2 \sin \alpha} \left\{ \sec^2 \theta/2 \sin^2 \alpha \cos \alpha - \sec^2 \theta/2 \cos \alpha \cos^2 \beta = 2 \cos \alpha \cos \theta \right\} \qquad \text{(A.14)}$$

$$\vec{e}_\alpha \cdot \vec{e}_x = - \sin \alpha \qquad \text{(A.15)}$$

and

$$\vec{e}_n \cdot \vec{e}_x = -1/2 \sec \theta/2 \cos \alpha \qquad \text{(A.16)}$$

From (A.1) we see that

$$\vec{e}_a \cdot \vec{e}_x = 2(\vec{e}_n \cdot \vec{e}_\alpha)(\vec{e}_n \cdot \vec{e}_x) - \vec{e}_\alpha \cdot \vec{e}_x \qquad \text{(A.17)}$$

Substituting (A.14), (A.15), and (A.16) in (A.17) we get:

$$\vec{e}_a \cdot \vec{e}_x = \frac{1}{2 \sin \alpha} \left\{ - \sec^2 \theta/2 \sin^2 \alpha \cos^2 \alpha + \sec^2 \theta/2 \cos^2 \alpha \cos^2 \beta + 2 \cos^2 \alpha \cos \theta + 2 \sin^2 \alpha \right\} \qquad \text{(A.18)}$$

Substituting $\sec^2 \theta/2 = 2/1 + \cos\theta$, (A.18) becomes

$$\vec{e_a} \cdot \vec{e_x} = \frac{1}{\sin\alpha\,(1+\cos\theta)}\Big\{\cos^2\alpha\,(\cos^2\theta - \sin^2\alpha + \cos^2\beta) + \cos\theta(\cos^2\alpha + \sin^2\alpha) + \sin^2\alpha\Big\} \tag{A.19}$$

But

$$\begin{aligned}\cos^2\theta - \sin^2\alpha + \cos^2\beta &= \cos^2\theta - 1 + \sin^2\theta\cos^2\phi + \sin^2\theta\sin^2\phi \\ &= \cos^2\theta - 1 + \sin^2\theta \\ &= 0\end{aligned} \tag{A.20}$$

Thus:

$$\vec{e_a} \cdot \vec{e_x} = \frac{\sin^2\alpha + \cos\theta}{\sin\alpha\,(1+\cos\theta)} = \frac{1 + \cos\theta - \sin^2\theta\cos^2\phi}{(1+\cos\theta)\sqrt{1 - \sin^2\theta\cos^2\phi}} \tag{A.21}$$

Let $\vec{e_a} \cdot \vec{e_x} = S$. Then for a minimum value of S, with θ held constant,

$$\frac{\partial S}{\partial\phi} = \frac{2\sin^2\theta\sin\phi\cos\phi}{(1+\cos\theta)\sqrt{1 - \sin^2\theta\cos^2\phi}}$$

$$-\frac{(1 + \cos\theta - \sin^2\phi\cos^2\phi)\sin^2\theta\sin\phi\cos\phi}{(1+\cos\theta)(1 - \sin^2\theta\cos^2\phi)^{3/2}} = 0 \tag{A.22}$$

or

$$2 - 2\sin^2\theta\cos^2\phi - 1 - \cos\theta + \sin^2\theta\cos^2\phi = 0. \tag{A.23}$$

Hence, for a minimum value of S

$$\sin^2\theta\cos^2\phi = 1 - \cos\theta. \tag{A.24}$$

Denoting by $S_m(\theta)$ the minimum value of S when θ is held constant, we find upon substituting (A.24) in (A.21) that

$$S_m(\theta) = \frac{2\cos\theta}{(1+\cos\theta)\sqrt{\cos\theta}} = \frac{2\sqrt{\cos\theta}}{1+\cos\theta} \tag{A.25}$$

Now

$$\frac{d}{d\theta}S_m(\theta) = \frac{-\sin\theta\,(1-\cos\theta)}{\sqrt{\cos\theta}\,(1+\cos\theta)^2} \leq 0 \text{ for } 0 \leq \theta < \pi/2 \tag{A.26}$$

Thus $S_m(\theta)$ is a steadily decreasing function of θ, and assumes its minimum value when θ takes on its maximum value Ω. Hence:

$$(\vec{e_a} \cdot \vec{e_x})_{min} = \frac{2\sqrt{\cos\Omega}}{1+\cos\Omega} \tag{A.27}$$

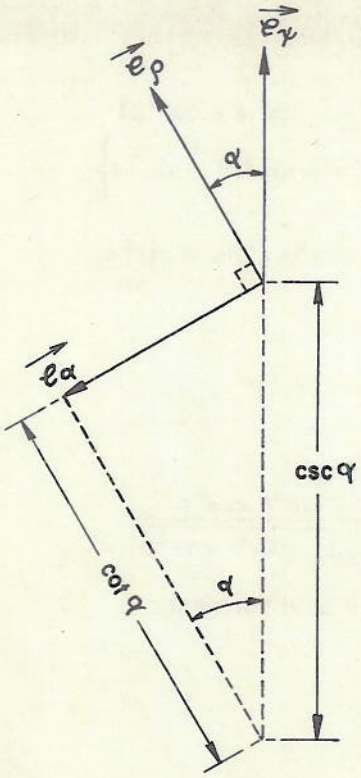

Fig. 17 - Relation Between $\vec{e}_\rho$, e_x, and $\vec{e}_\alpha$

The following table illustrates how little $\vec{e}_a \cdot \vec{e}_x$ differs from unity over the aperture.

Ω	30°	45°	52°	60°
$(\vec{e}_a \cdot \vec{e}_x)_{min}$	0.997	0.985	0.972	0.943

* * *

APPENDIX B

Calculation of Secondary E- and H-Plane Sum and Difference Patterns

We shall first express the vector $\vec{N}$ given by equation (14) as an integral in terms of spherical coordinates. If r and ϕ represent the polar coordinates of a point in the aperture plane, then

$$da = r\, dr\, d\phi \tag{B.1}$$

and

$$r = \rho \sin\theta \tag{B.2}$$

The equation of the paraboloid in spherical coordinates is given by

$$\rho = f \sec^2 \theta/2 \tag{B.3}$$

Hence

$$r = f \sec^2\theta/2 \sin\theta = 2f \tan\theta/2 \tag{B.4}$$

and

$$da = 2f \tan\theta/2 \cdot f \sec^2\theta/2\, d\theta\, d\phi = 2f^2 \tan\theta/2 \sec^2\theta/2\, d\theta\, d\phi \tag{B.5}$$

Also

$$x = \rho \sin\theta \cos\phi \tag{B.6}$$

$$y = \rho \sin\theta \sin\phi \tag{B.7}$$

Substituting (B.5), (B.6), (B.7), and (11) into (14), we get

$$\vec{N} = \vec{e_x}\, e^{-jk2f} \int_0^{\Omega}\int_0^{2\pi} \frac{F(\theta,\phi)}{f \sec^2\theta/2}\, 2f^2 \tan\theta/2 \sec^2\theta/2\, e^{jk\rho \sin\theta \sin\psi \cos(\phi - \xi)} d\phi\, d\theta \tag{B.8}$$

$$= \vec{e_x}\, 2f\, e^{-jk2f} \int_0^{\Omega}\int_0^{2\pi} F(\theta,\phi) \tan\theta/2\, e^{jk2f \tan\theta/2 \sin\psi \cos(\phi - \xi)} d\phi\, d\theta \tag{B.9}$$

For large apertures the main portion of the radiation pattern will be confined to small values of ψ. But for small values of ψ, $1 + \cos\psi \cong 2$. Since $N_y = 0$, we find upon substituting (B.8) in (12) and (13) that for small values of ψ we have very nearly:

$$E_{p\psi}(\psi,\xi) = jkf/\pi\, e^{-jk(R + 2f)} \cos_{\xi} \int_0^{\Omega}\int_0^{2\pi} F(\theta,\phi) \tan\theta/2\, e^{jk2f \tan\theta/2 \sin\psi \cos(\phi - \xi)} d\phi d\theta \tag{B.10}$$

$$E_p(\psi,\xi) = -jk/\pi\, e^{-jk(R + 2f)} \sin_{\xi} \int_0^{\Omega}\int_0^{2\pi} F(\theta,\phi) \tan\theta/2\, e^{jk2f \tan\theta/2 \sin\psi \cos(\phi - \xi)} d\phi d\theta \tag{B.11}$$

To obtain the E-plane pattern we substitute $\xi = 0$ in (B.10) and (B.11), and since $E_{p\xi}(\psi,0) \equiv 0$, we see that the E-plane pattern is given by $E_{p\psi}(\psi,0)$. To determine the H-plane pattern we substitute $\xi = \pi/2$. In this case $E_{p\psi}(\psi,\pi/2) \equiv 0$, and therefore the H-plane pattern is given by $E_{p\xi}(\psi,\pi/2)$. The patterns obtained are for an arbitrary feed pattern represented by the function $F(\theta,\phi)$ which appears on the right side of (B.10) and (B.11). If for $F(\theta,\phi)$ we substitute the appropriate sum and difference patterns of the feed, we then obtain the corresponding secondary sum and difference patterns of the antenna as a whole. Let us omit the common phase factor $j\, e^{-jk(R + 2f)}$ which appears in each of the expressions for the E- and H-plane patterns, and denote the resulting functions by $E_{es}(\psi)$, $E_{hs}(\psi)$, $E_{ed}(\psi)$, and $E_{hd}(\psi)$ where $E_{es}(\psi)$ and $E_{hs}(\psi)$ represent the E- and H-plane sum patterns respectively, and $E_{ed}(\psi)$ and $E_{hd}(\psi)$ represent the E- and H-plane difference patterns respectively. If for $F(\theta,\phi)$ we now substitute the functions $K_1 e'_s(\theta,\phi)$, $K_2 e'_e(\theta,\phi)$, and $K_3 e'_h(\theta,\phi)$, and if we let

$$u = 2f \tan \theta/2 \tag{B.12}$$

we find that:

$$E_{es}(\psi) = K_1 kf/\pi \int_0^{\Omega} \int_0^{2\pi} e'_s(\theta,\phi) \tan \theta/2\, e^{jku \sin \psi \cos \phi}\, d\phi\, d\theta \tag{B.13}$$

$$E_{hs}(\psi) = K_1 kf/\pi \int_0^{\Omega} \int_0^{2\pi} e'_s(\theta,\phi) \tan \theta/2\, e^{jku \sin \psi \sin \phi}\, d\phi\, d\theta \tag{B.14}$$

$$E_{ed}(\psi) = K_2 kf/\pi \int_0^{\Omega} \int_0^{2\pi} e'_e(\theta,\phi) \tan \theta/2\, e^{jku \sin \psi \cos \phi}\, d\phi\, d\theta \tag{B.15}$$

$$E_{hd}(\psi) = K_3 kf/\pi \int_0^{\Omega} \int_0^{2\pi} e'_h(\theta,\phi) \tan \theta/2\, e^{jku \sin \psi \sin \phi}\, d\phi\, d\theta \tag{B.16}$$

Let us now consider the functions $e'_s(\theta,\phi)$, $e'_e(\theta,\phi)$, and $e'_h(\theta,\phi)$. From equations (1), (2), and (3) we see that if we let $a = b$, each of these functions can be expressed in the following form

$$\left.\begin{matrix} e'_s \\ e'_e \\ e'_h \end{matrix}\right\} = e(\theta,\phi)\, \Sigma \pm e^{\frac{jka \sin \theta}{2}(\sigma \cos \phi + \tau \sin \phi)} \tag{B.17}$$

where

$$\sigma = \pm 1, \text{ and } \tau = \pm 1.$$

To simplify the problem further we shall expand the function $e(\theta,\phi)$ in a Fourier series with respect to ϕ, and retain the first two terms in the expansion. The pattern of a single horn is symmetric with respect to the two principal planes; that is

$$e(\theta,\phi) = e(\theta,-\phi) \qquad e(\theta,\phi) = e(\theta,\, \pi - \phi)$$

Hence the Fourier series will contain only cosine terms of even multiples of ϕ and we may write

$$e(\theta,\phi) = A_0(\theta) + A_2(\theta) \cos 2\phi \tag{B.18}$$

Substituting $\phi = 0$ and $\pi/2$ respectively, and making use of the notation introduced in (6a) and (6b) we have

$$e(\theta) = A_0(\theta) + A_2(\theta) \tag{B.19}$$

$$h(\theta) = A_0(\theta) - A_2(\theta) \tag{B.20}$$

Thus

$$A_0(\theta) = 1/2\left\{e(\theta) + h(\theta)\right\} \tag{B.21}$$

$$A_2(\theta) = 1/2\left\{e(\theta) - h(\theta)\right\} \tag{B.22}$$

We shall see later that the contribution to the integrals in equations (B.13) - (B.16) inclusive due to the second term in the right side of (B.18) is small compared to the contribution of the first term. Thus, the patterns are determined essentially by the arithmetic mean of the E- and H-plane patterns of the single horns.

Substitution of equations (B.17) and (B.18) into equations (B.13) - (B.16) inclusive, leads to the evaluation of the following integrals:

$$L_e(\sigma,\tau,\theta,\psi) = \int_0^{2\pi} e^{jk\left\{\frac{a}{2}\sin\theta(\sigma\cos\phi + \tau\sin\phi) + u\sin\psi\cos\phi\right\}} d\phi \tag{B.23}$$

$$L_h(\sigma,\tau,\theta,\psi) = \int_0^{2\pi} e^{jk\left\{\frac{a}{2}\sin\theta(\sigma\cos\phi + \tau\sin\phi) + u\sin\psi\sin\phi\right\}} d\phi \tag{B.24}$$

$$M_e(\sigma,\tau,\theta,\psi) = \int_0^{2\pi} \cos 2\phi\, e^{jk\left\{\frac{a}{2}\sin\theta(\sigma\cos\phi + \tau\sin\phi) + u\sin\psi\cos\phi\right\}} d\phi \tag{B.25}$$

$$M_h(\sigma,\tau,\theta,\psi) = \int_0^{2\pi} \cos 2\phi\, e^{jk\left\{\frac{a}{2}\sin\theta(\sigma\cos\phi + \tau\sin\phi) + u\sin\psi\sin\phi\right\}} d\phi \tag{B.26}$$

Substituting $\sigma = \tau = 1$ in (B.25) gives:

$$L_e(1,1,\theta,\psi) = \int_0^{2\pi} e^{jk\frac{a}{2}\sin\theta(\cos\phi + \sin\phi) + u\sin\psi\cos\phi} d\phi \tag{B.27}$$

If we let $\phi = -t$ in this integral we get

$$L_e(1,1,\theta,\psi) = \int_0^{2\pi} e^{jk\frac{a}{2}\sin\theta(\cos t - \sin t) + u\sin\psi\cos t}\, dt$$

$$= L_e(1,-1,\theta,\psi) \tag{B.28}$$

Substituting $\phi = t + \pi$ in (B.27) gives

$$L_e(1,1,\theta,\psi) = \int_0^{2\pi} e^{jk\frac{a}{2}\sin\theta(-\cos t - \sin t) - u\sin\psi\cos t}\, dt$$

$$= L_e(-1,-1,\theta,-\psi) \tag{B.29}$$

Substituting $\phi = \pi - t$ in (B.27) gives

$$L_e(1,1,\theta,\psi) = \int_0^{2\pi} e^{jk\frac{a}{2}\sin\theta(-\cos t + \sin t) - u\sin\psi\cos t}\, dt$$

$$= L_e(-1,1,\theta,-\psi) \tag{B.30}$$

It follows from equations (B.28), (B.29) and (B.30) that

$$L_e(1,1,\theta,\psi) + L_e(1,-1,\theta,\psi) + L_e(-1,1,\theta,\psi) + L_e(-1,-1,\theta,\psi)$$

$$= 2\left\{L_e(1,1,\theta,\psi) + L_e(1,1,\theta,-\psi)\right\} \tag{B.31}$$

and

$$L_e(1,1,\theta,\psi) + L_e(1,-1,\theta,\psi) - L_e(-1,1,\theta,\psi) - L_e(-1,-1,\theta,\psi)$$

$$= 2\left\{L_e(1,1,\theta,\psi) - L_e(1,1,\theta,-\psi)\right\} \tag{B.32}$$

In a similar manner it can be shown that equations (B.31) and (B.32) remain valid if the function L_e is replaced by L_h, M_e, or M_h. It can also be shown that

$$L_h(1,1,\theta,\psi) = L_e(1,1,\theta,\psi) \tag{B.33}$$

and

$$M_h(1,1,\theta,\psi) = M_e(1,1,\theta,\psi) \tag{B.34}$$

Now let the functions $P(\psi)$ and $Q(\psi)$ be defined as follows:

$$P(\psi) \equiv \int_0^{\Omega} A_o(\theta)\tan\theta/2\; L_e(1,1,\theta,\psi)\, d\theta \tag{B.35}$$

$$Q(\psi) = \int_0^{\Omega} A_2(\theta) \tan \theta/2 \; M_e(1,1,\theta,\psi) \, d\theta \qquad \text{(B.36)}$$

If the results of equations (B.17) - (B.36) inclusive, are substituted in equations (B.13) - (B.16) inclusive, we get:

$$E_{es}(\psi) = 2K_1 kf/\pi \left\{P(\psi) + P(-\psi) + Q(\psi) + Q(-\psi)\right\} \qquad \text{(B.37)}$$

$$E_{hs}(\psi) = 2K_1 kf/\pi \left\{P(\psi) + P(-\psi) - Q(\psi) - Q(-\psi)\right\} \qquad \text{(B.38)}$$

$$E_{ed}(\psi) = 2K_2 kf/\pi \left\{P(\psi) - P(-\psi) + Q(\psi) - Q(-\psi)\right\} \qquad \text{(B.39)}$$

$$E_{hd}(\psi) = 2K_3 kf/\pi \left\{P(\psi) - P(-\psi) - Q(\psi) + Q(-\psi)\right\} \qquad \text{(B.40)}$$

Let us now consider the functions $L_e(1,1,\theta,\psi)$ and $M_e(1,1,\theta,\psi)$. Let

$$v = \sqrt{\left(\frac{a}{2}\sin\theta + u \sin\psi\right)^2 + \left(\frac{a}{2}\sin\theta\right)^2} \qquad \text{(B.41)}$$

and

$$\eta = \tan^{-1}\left(\frac{a}{2}\sin\theta + u\sin\psi\right)\Big/\left(\frac{a}{2}\sin\theta\right) \qquad \text{(B.42)}$$

Then

$$L_e(1,1,\theta,\psi) = \int_0^{2\pi} e^{jk\left\{\left(\frac{a}{2}\sin\theta\right)\sin\phi + \left(\frac{a}{2}\sin\theta + u\sin\psi\right)\cos\phi\right\}} d\phi$$

$$= \int_0^{2\pi} e^{jkv\sin(\phi+\eta)} \, d\phi$$

$$= 2\pi J_0(kv) \qquad \text{(B.43)}$$

and similarly

$$M_e(1,1,\theta,\psi) = \int_0^{2\pi} \cos 2\phi \; e^{jkv\sin(\phi+\eta)} \, d\phi$$

$$= \int_0^{2\pi} \cos(2\phi - 2\eta) \; e^{jkv\sin\phi} \, d\phi$$

$$= 2\pi \cos 2\eta \; J_2(kv) \qquad \text{(B.44)}$$

where

$$\cos 2\eta = 2\cos^2\eta - 1 = (a\sin\theta)^2/2v^2 - 1 \qquad \text{(B.45)}$$

Thus

$$P(\psi) = 2\pi \int_0^{\Omega} A_o(\theta) \tan \theta/2 \, J_o(kv) \, d\theta \tag{B.46}$$

$$Q(\psi) = 2\pi \int_0^{\Omega} A_2(\theta) \tan \theta/2 \cos 2\eta \, J_2(kv) \, d\theta \tag{B.47}$$

Equations (B.46) and (B.47) together with equations (B.37) - (B.40) inclusive, determine the secondary E- and H-plane sum and difference patterns.

To obtain a series expansion for the secondary patterns let:

$$t = \pi D \sin \psi/2\lambda \tag{B.48}$$

$$s = 4f/D \tan \theta/2 \tag{B.49}$$

$$p = \sqrt{2}\,\pi \, a \sin \theta/\lambda \tag{B.50}$$

If $2\pi/\lambda$ is substituted for k, then

$$L_e(1,1,\theta,\psi) = \int_0^{2\pi} e^{j\pi \, a/\lambda \sin \theta(\cos \phi + \sin \phi)} \cdot e^{j4\pi \, f/D \tan \theta/2 \, D/\lambda \sin \psi \cos \phi} \, d\phi$$

$$= \int_0^{2\pi} e^{jp \sin \left(\phi + \frac{\pi}{4}\right)} e^{j2st \cos \phi} \, d\phi$$

$$= \sum_{n=0}^{\infty} s^n t^n \frac{(2j)^n}{n!} \int_0^{2\pi} e^{jp \sin \left(\phi + \frac{\pi}{4}\right)} \cos^n \phi \, d\phi \tag{B.51}$$

or

$$L_e(1,1,\theta,\psi) = \sum_{n=0}^{\infty} s^n t^n \frac{(2j)^n}{n!} \int_0^{2\pi} \cos^n \phi \left\{ J_o(p) + 2 \sum_{m=1}^{\infty} J_{2m}(p) \cos 2m \left(\phi + \frac{\pi}{4}\right) \right.$$

$$\left. + 2j \sum_{m=0}^{\infty} J_{2m+1}(p) \sin (2m+1) \left(\phi + \frac{\pi}{4}\right) \right\} d\phi$$

$$= 2\pi \sum_{n=0}^{\infty} (-1)^n \frac{s^{2n} t^{2n}}{(2n)!} \left\{ C_n^{2n} J_o(p) + 2 \sum_{m=1}^{n} C_{n-m}^{2n} J_{2m}(p) \cos m\pi/2 \right\}$$

$$+ 4\pi \sum_{n=0}^{\infty} (-1)^{n+1} \frac{s^{2n+1} t^{2n+1}}{(2n+1)!} \left\{ \sum_{m=0}^{n} C_{n-m}^{2n+1} J_{2m+1}(p) \sin (2m+1)\pi/4 \right\} \tag{B.52}$$

where

$$C_m^n = \frac{n!}{m!\,(n-m)!} \quad 0 \leq m \leq n$$

$$= 0 \qquad \text{if } m < 0, \text{ or } m > n$$

Similarly

$$M_e(1,1,\theta,\psi) = \int_0^{2\pi} \cos 2\phi \; e^{jp \sin\left(\phi + \frac{\pi}{4}\right)} e^{jst \cos \phi} \, d\phi$$

$$= \sum_{n=0}^{\infty} s^n t^n \frac{(2j)^n}{n!} \int_0^{2\pi} \cos 2\phi \cos^n \phi \left\{ J_0(p) + 2 \sum_{m=1}^{\infty} \right.$$

$$\left. J_{2m}(p) \cos 2m\left(\phi + \frac{\pi}{4}\right) + 2j \sum_{m=0}^{\infty} J_{2m+1}(p) \sin(2m+1)\left(\phi + \frac{\pi}{4}\right) \right\} d\phi$$

$$= \pi \sum_{n=0}^{\infty} (-1)^n \frac{s^{2n} t^{2n}}{(2n)!} \left\{ \left(C_{n+1}^{2n+2} - 2C_n^{2n} \right) J_0(p) \right.$$

$$\left. + 2 \sum_{m=1}^{n+1} \left(C_{n+1-m}^{2n+2} - 2C_{n-m}^{2n} \right) \cos \frac{m\pi}{2} J_{2m}(p) \right\}$$

$$+ 2\pi \sum_{n=0}^{\infty} (-1)^{n+1} \frac{s^{2n+1} t^{2n+1}}{(2n+1)!} \left\{ \sum_{m=0}^{n+1} \left(C_{n+1-m}^{2n+3} - 2C_{n-m}^{2n+1} \right) \right.$$

$$\left. \sin(2m+1) \frac{\pi}{4} J_{2m+1}(p) \right\} \tag{B.53}$$

Substituting (B.52) and (B.53) in (B.35) and (B.36) respectively, and recalling that $4f/D = \cot \Omega/2$, we get

$$8f/D \; P(\psi) = \sum_{n=0}^{\infty} a_n t^n \tag{B.54}$$

$$8f/D\ Q(\psi) = \sum_{n=0}^{\infty} b_n t^n \qquad \text{(B.55)}$$

where

$$a_{2n} = (-1)^n\, 4\pi(\cot\ \Omega/2)^{2n+1} \int_0^{\Omega} A_o(\theta)\ (\tan\ \theta/2)^{2n+1}$$

$$\left\{ \frac{J_o(p)}{(n!)^2} + 2 \sum_{m=1}^{n} \frac{\cos \frac{m\pi}{2}\, J_{2m}(p)}{(n-m)!\,(n+m)!} \right\} d\phi$$

$$a_{2n+1} = (-1)^{n+1}\, 8\ \pi(\cot\ \Omega/2)^{2n+2} \int_0^{\Omega} A_o(\theta)\ (\tan\ \theta/2)^{2n+2}$$

$$\left\{ \sum_{m=0}^{n} \frac{\sin(2m+1)\frac{\pi}{4} J_{2m+1}(p)}{(n-m)!\,(n-m+1)!} \right\} d\theta \qquad \text{(B.56)}$$

$$b_{2n} = (-1)^n\, 4\pi(\cot\ \Omega/2)^{2n+1} \int_0^{\Omega} A_o(\theta)\ (\tan\ \theta/2)^{2n+2}$$

$$\left\{ \frac{J_o(p)}{(n-1)!\,(n+1)!} + 2 \sum_{m=1}^{n+1} \frac{(n^2+n+m^2) \cos m\frac{\pi}{2} J_{2m}(p)}{(n+1-m)!\,(n+1+m)!} \right\} d\theta$$

$$b_{2n+1} = (-1)^{n+1}\ 8\pi(\cot \Omega/2)^{2n+2} \int_0^{\Omega} A_2(\theta)\ (\tan\ \theta/2)^{2n+2}$$

$$\left\{ \sum_{m=0}^{n+1} \frac{\left[(n+1)^2 + m + m^2\right] \sin(2m+1)\frac{\pi}{4} J_{2m+1}(p)}{(n+1-m)!\,(n+2+m)!} \right\} d\theta \qquad \text{(B.57)}$$

Substituting (B.54) and (B.55) in (B.37) – (B.40) inclusive gives equations (18a) – (18d) inclusive for the secondary patterns.

* * *

APPENDIX C

Variation of Secondary Patterns with a/λ

The E-plane patterns only will be considered. The H-plane patterns can be handled in the same way.

Denote by $E_e(\psi)$ either of the two E-plane patterns with the phase factor $je^{-jk(R + 2f)}$ omitted. Substituting $\xi = 0$ in (B.10) and (B.11), and replacing Ω by ω, it is seen that

$$E_e(\psi) = 2kf/\pi \int_0^{\omega} \tan \theta/2 \, d\theta \int_0^{2\pi} F(\theta,\phi) \, e^{jk2f \tan \theta/2 \sin \psi \cos \phi} \, d\phi \qquad (C.1)$$

The function $F(\theta,\phi)$ represents the field strength sum or difference pattern of the 4-horn feed, as the case may be. To emphasize the dependence on the parameters a/λ and ω, (C.1) may be rewritten as follows:

$$E_e(\psi,a/\lambda,\omega) = 4f/\lambda \int_0^{\omega} \tan \theta/2 \, d\theta \int_0^{2\pi} F(\theta,\phi,a/\lambda) \, e^{j4f/\lambda \tan \theta/2 \sin \psi \cos \phi} \, d\phi \qquad (C.2)$$

Since $4f/D = \cot \omega/2$, (C.2) may be written as

$$E_e(\psi,a/\lambda,\omega) = D/\lambda \cot \omega/2 \int_0^{\omega} \tan \theta/2 \, d\theta \int_0^{2\pi} F(\theta,\phi,a/\lambda) \, e^{j \tan \theta/2 \cot \omega/2 \, \pi D/\lambda \sin \psi \cos \phi} \, d\phi \qquad (C.3)$$

If $\omega/2$ is not very large, and if a/λ lies between limits which do not differ greatly from unit, then

$$\cot \omega/2 \tan \theta/2 = \frac{\tan \theta/2}{\tan \omega/2} \cong \frac{\tan a\theta/2\lambda}{\tan a\omega/2\lambda} = \cot a\omega/2\lambda \tan a\theta/2\lambda \qquad (C.4)$$

From the previous discussion of the primary patterns of the 4-horn feed it can be seen that, apart from a scale factor, the patterns for various values of a/λ can be represented by a single function of $a\theta/\lambda$ and ϕ, say $U(a\theta/\lambda,\phi)$. The scale factor will depend only on the gain of the feed. If it is assumed that the gain of the feed is proportional to $(a/\lambda)^2$, then

$$F(\theta,\phi,a/\lambda) = K \, a/\lambda \, U(a\theta/\lambda,\phi) \qquad (C.5)$$

where K is a constant independent of a/λ.

Substituting (C.4) and (C.5) in (C.3) gives

$$E_e(\psi,a/\lambda,\omega) = D/\lambda \cot a\omega/2\lambda \int_0^{\omega} \tan a\theta/2\lambda \, d\theta \int_0^{2\pi} Ka/\lambda \, U(a\theta/\lambda,\phi) \, e^{j \tan a\theta/2\lambda \cot a\omega/2\lambda \, \pi D/\lambda \sin \psi \cos \phi} \, d\phi \qquad (C.6)$$

Substituting $a\theta/\lambda = \bar{\theta}$, and $a\omega/\lambda = \Omega$, (C.6) becomes

$$E_e(\psi, a/\lambda, \omega) = K\, D/\lambda \cot \Omega/2 \int_0^{\Omega} \tan \bar{\theta}/2 \, d\bar{\theta} \int_0^{2\pi} U(\bar{\theta}, \phi)$$

$$e^{j \tan \bar{\theta}/2 \cot \Omega/2 \, \pi D/\lambda \sin \psi \cos \phi} \, d\phi \qquad \text{(C.7)}$$

$$= E_e(\psi, \Omega)$$

The expression on the right side of (C.7) is precisely the expression for the secondary pattern of an antenna with feed pattern given by $U(\theta,\phi)$ and a reflector which subtends an angle 2Ω at the focus. Now if both a/λ and ω are allowed to vary, the resulting pattern is given by (C.7) in which only $\Omega = a\omega/\lambda$ varies. Thus, within the limits of the approximations that have been made, a study of the variation in secondary patterns, when a/λ and ω are both varied is equivalent to a study of the case where a/λ is held fixed and only Ω is varied, which is the case that has been treated in this report. It should be kept clearly in mind that throughout the discussion D/λ is considered to be constant.

* * *

REFERENCES

1. Page, R. M., "Accurate Angle Tracking by Radar," NRL Report No. RA 3A 222A, Confidential, December 1944.

   Trevor, J.B. and Hastings, A.E., "Analysis and Specifications of Simultaneous Lobing System (TAB)," NRL Report No. R-2554, Confidential, July 1945.

   Hearn, Claude E., "A Study of the Range Performance of a Multilobe Tracking Radar," G. E. Report No. 55309, Confidential, April 1947.

   Winn, Oliver H., "Analysis of Monopulse Radar Tracking System," Report No. E.D.G. 30634-1, Confidential, October 1947.

   Martin, J.F.P., "Radiation Characteristics of Certain Antenna Systems for Angle Tracking," BTL Report No. MM-2730-7, Confidential, January 1947.

   Hastings, A. E., "Antenna Feeds for Tracking Radar," NRL Report No. R-3268, Confidential, March 1948.

   Gerwin, H. L., "Simultaneous Lobing Radar (TAB)," NRL Progress Report, Confidential, July 1948.

   Quigley, E., Riblet, H. J., and Saad, T., "Compact Simultaneous Lobing Circuit," NRL Report No. R-3341, Confidential, November 1948.

2. Risser, J. R., "Characteristics of Horn Feeds on Rectangular Waveguide," Radiation Lab. Report No. 656, December 1945.

3. Silver, S., "Microwave Antenna Theory and Design," Radiation Lab. Series, McGraw-Hill, Ch. V, p. 162, (111a), (111b), 1949.

4. Ch. V, p. 144, (56a).

* * *

PRNC-2200-8-15-49-150